Food Microbiology 82 (2019) 177–193

Contents lists available at ScienceDirect

Food Microbiology

journal homepage: www.elsevier.com/locate/fm

Proteomic analysis of the food spoiler *Pseudomonas fluorescens* ITEM 17298 reveals the antibiofilm activity of the pepsin-digested bovine lactoferrin

Laura Quintieri[a,*], Daniela Zühlke[b], Francesca Fanelli[a], Leonardo Caputo[a], Vania Cosma Liuzzi[a], Antonio Francesco Logrieco[a], Claudia Hirschfeld[b], Dörte Becher[b], Katharina Riedel[b]

[a] National Research Council of Italy, Institute of Sciences of Food Production, (CNR-ISPA), Via G. Amendola 122/O, 70126, Bari, Italy
[b] Institute of Microbiology, University of Greifswald, Greifswald, D-17487, Germany

ARTICLE INFO

Keywords:
Food spoilers
Pigments
Temperature adaptation
Antimicrobial peptides
Genomics
GeLC-MS/MS

ABSTRACT

Pseudomonas fluorescens is implicated in food spoilage especially under cold storage. Due to its ability to form biofilm *P. fluorescens* resists to common disinfection strategies increasing its persistance especially across fresh food chain. Biofilm formation is promoted by several environmental stimuli, but gene expression and protein changes involved in this lifestyle are poorly investigated in this species.

In this work a comparative proteomic analysis was performed to investigate metabolic pathways of underlying biofilm formation of the blue cheese pigmenting *P. fluorescens* ITEM 17298 after incubation at 15 and 30 °C; the same methodology was also applied to reveal the effects of the bovine lactoferrin hydrolysate (HLF) used as antibiofilm agent.

At 15 °C biofilm biomass and motility increased, putatively sustained by the induction of regulators (PleD, AlgB, CsrA/RsmA) involved in these phenotypic traits. In addition, for the first time, TycC and GbrS, correlated to indigoidine synthesis (blue pigment), were detected and identified. An increase of virulence factors amounts (leukotoxin and PROKKA_04561) were instead found at 30 °C. HLF caused a significant reduction in biofilm biomass; indeed, at 15 °C HLF repressed PleD, TycC and GbrS and induced the negative regulators of alginate biosynthesis; at both temperatures induced the cyclic-di-GMP-binding biofilm dispersal mediator (PROKKA_02061).

In conclusion, in this work protein determinats of biofilm formation were revelead in ITEM 17298 under the low temperature; the synthesis of these latter were inhibited by HLF confirming its possible exploitation as antibiofilm agent for biotechnological applications in cold stored foods.

1. Introduction

Pseudomonas fluorescens are widespread psychrotrophic Gram-negative bacteria implicated in food spoilage, especially under cold storage, causing the reduction of shelf-life and loss of foodstuffs (Baruzzi et al., 2012; Caldera et al., 2016). *Pseudomonas* spp. contaminations in food chain are mostly derived from water and pipe surfaces where these bacteria grow as biofilms (Srey et al., 2013). During biofilm formation, the transition from planktonic (free living) cells to the attached aggregated form is triggered by *de-novo* expression of transcriptional regulators and key genes responsible for surface-cell and intracellular interactions, metabolic pathways, virulence and resistance mechanisms (Waite et al., 2005). Moreover, the formation of a biofilm is considered a strategy to counteract microbial competition (Oliveira et al., 2015).

Biofilm formation can be influenced and promoted by different factors, such as nutrients, kind of surfaces, stress response (Monds and O'Toole, 2009). Recently, a positive correlation between low temperatures and biofilm production by foodborne *P. fluorescens* was found by Rossi et al. (2018) reporting that the number of biofilm-forming strains at 15 °C was higher than that at 30 °C. Likewise, Chierici et al. (2016) and Caputo et al. (2015) reported that low temperatures (4 and 15 °C) induced pigment production for this bacterial species. In *P. aeruginosa* the role of pigments in biofilm formation (Mavrodi et al., 2013; Park et al., 2014), as well as other genes and factors involved in the transition to aggregated cells and biofilm maintenance has been studied for a long time. By contrast, to the best of our knowledge, no metabolic pathways have been deeply investigated to explain *P. fluorescens* responses to environmental conditions. After all, the human risks correlated with the spread of this species had been underestimated. It is only recently that some studies identified *P. fluorescens* in clinical

* Corresponding author.
E-mail address: laura.quintieri@ispa.cnr.it (L. Quintieri).

https://doi.org/10.1016/j.fm.2019.02.003
Received 18 September 2018; Received in revised form 4 February 2019; Accepted 6 February 2019
Available online 08 February 2019
0740-0020/

environment (Dickson et al., 2014; Nishimura et al., 2017) and correlated them to human diseases (Madi et al., 2010; Nishimura et al., 2017). In addition to this, *P. fluorescens* harbors an enormous pool of antibiotic and biocide resistance genes that can be transmitted to human and animals via horizontal gene transfer through contaminated foods (Donnarumma et al., 2010; Naghmouchi et al., 2012). It is clear that these results highlighted the urgent need for further researches to better characterize and counteract the spread of this microorganism.

In this regard, several strategies preventing biofilm formation have been investigated and also identified from diverse natural sources, such as plant-derived compounds (Hentzer et al., 2003; Caputo et al., 2018). In this context, the application of natural cationic peptides was reported as a promising antibiofilm strategy against different species (Rajput and Kumar, 2018); however, biophysical properties required for antibiofilm activity and its mechanism are not fully known.

In our previous works, we investigated the antimicrobial efficacy of bovine lactoferrin-derived peptides (BLFPs) in counteracting the growth of foodborne pseudomonads (Quintieri et al., 2012, 2013a); the antimicrobial efficacy of these peptides was demonstrated *in vitro,* in cold stored foods and on functionalized coatings (Baruzzi et al., 2015; Quintieri et al., 2013b, 2015); BLFPs were also able to block the blue discoloration of Mozzarella cheese contaminated by the pigmenting *P. fluorescens* ITEM 17298 (Caputo et al., 2015). Studies by other authors showed that peptides derived from human lactoferrin significantly inhibited these phenotypic traits also in other microorganisms (Morici et al., 2016; Xu et al., 2010; Sánchez-Gómez et al., 2015); however, no results revealed how these compounds act.

Therefore, in this work we firstly investigated the ability of the pigmenting *P. fluorescens* ITEM 17298 to form biofilm under two temperatures (15 °C and 30 °C); then, we present a comparative proteomic analysis of *P. fluorescens* ITEM 17298 planktonic cells, grown under the assayed temperatures in order to reveal metabolic pathways and physiological changes that characterize strain adaptation to these conditions. In addition to this, the same methodology was applied on the planktonic cells treated with bovine lactoferrin hydrolysate (HLF) acting as “antibiofilm agent” at its sub-lethal concentration. The results of this study reveal some protein targets and metabolic pathways involved in the expression of biofilm phenotype at the assayed temperatures and affected by peptide treatment.

2. Material and methods

2.1. Bacterial strain, growth conditions and genome analysis

The foodborne *Pseudomonas fluorescens* ITEM 17298 (previously named as 84095) from the ISPA-CNR microbial collection (http://server.ispa.cnr.it/ITEM/Collection/; Fanelli et al., 2017) was freshly streaked onto Luria Bertani agar (LB broth: 10.0 g of tryptone, 5.0 g of yeast extract, 10.0 g of NaCl per liter added with 16 g/L of technical agar, Sigma-Aldrich, Milan, Italy) and grown overnight at 30 °C. After incubation a single colony was inoculated into LB broth (5 mL) and incubated overnight (30 °C, 150 rpm) in order to be used for the subsequent experiments.

Draft genome sequence was performed as reported by Fanelli et al. (2017) and it was deposited in Genbank under the accession number NPKB00000000. Contigs were annotated using Prokka pipeline implemented in the Galaxy platform (Seemann, 2014). UniProtKB AC/ID identifiers retrieved by PFAM annotator tools were mapped against the PSEUDOCAP database and used to categorize genes in functional classes (Winsor et al., 2010).

2.2. Static biofilm formation and motility assays under two temperatures

Biofilm formation was assayed in 96-well microtiter plates (Corning®, NY, USA) and quantified as described by O'Toole (2011). Briefly, overnight cultures of *P. fluorescens* ITEM 17298 were diluted 1:100 into fresh LB (100 µL; 8 biological replicates for each timepoint sampling) and incubated at 15 and 30 °C for 48 h. Not inoculated LB was used as negative control. At 24 and 48 h, planktonic cell growth was determined by measuring optical density (OD) at 600 nm with a microplate reader (Varioskan Flash, Thermo Fisher, Milan, Italy); then, planktonic cells were carefully removed and wells were washed twice with distilled water; biofilm cells adhering to the bottom and side of each well were stained with crystal violet (CV; 0.1%, w/v). After a second washing step, biofilm-associated crystal violet was solubilized with 30% acetic acid (v/v) and its optical density was measured at 570 nm.

Swarming and swimming motility assays were performed in Petri dishes (polystyrene, diameter of 50 mm) containing 10 mL of LB (Khan et al., 2009) solidified with 0.5 and 0.3% (w/v) of agar, respectively. Swim and swarm plates were inoculated with 2.5 µL of bacterial broth culture representing approximately 1×10^8 CFU/mL (corresponding to 0.3 OD_{600nm}; Caputo et al., 2015). The swarming assay was carried out placing this inoculum volume on the agar surface at the center of the plate. Instead, for the swimming assay, the inoculum was placed directly in the center of the thickness of the agar. All plates were incubated at 15 and 30 °C. The diameters of the swarming and swimming motility zones were measured at 24, 48 and 72 h of incubation. By contrast, twitching motility was evaluated on LB medium supplemented with 1% agar (w/v) (Deziel et al., 2001). Bacterial cells were inoculated at the bottom of the agar-dish interface. The plates were incubated at 15 and 30 °C. At selected times (24, 48, 72 h), the agar layer was carefully removed, and the plates were stained with 0.1% of CV (w/v). After washing step biofilm was solubilized and quantified as described above.

2.3. Effect of HLF treatment on motility and biofilm formation: determination of the minimum biofilm inhibitory concentration (MBIC)

Freeze-dried HLF was obtained by hydrolysis of BLF with pepsin according to Quintieri et al. (2012). Then, overnight cultures of *P. fluorescens* ITEM 17298 were inoculated, in triplicate, at a final concentration of *ca.* 3 log CFU/mL in sterile Falcon(R) 6 wells polystyrene microplates (BD Biosciences, Erembodegem, Belgium) filled with 5 mL of LB (control) and LB with increasing concentration of HLF (1.5, 3, 6, 12 mg/mL). Microplates were incubated at 15 and 30 °C for 48 h. Microbial counts were determined at 7, 24, 32 and 48 h by plating serial 10-fold dilutions on LB agar (LB amended with 16 g/L of technical agar). Subsequently, sub-lethal HLF concentrations which did not cause any significant changes in viable cell count, were assayed for the inhibition of biofilm development in 6 wells polystyrene microplates (O'Toole, 2011). The Minimum Biofilm Inhibitory Concentration (MBIC) was determined as the HLF concentration needed to reduce biofilm biomass by more than 50% (HLF-MBIC). At the end of incubation (48 h), planktonic cells, grown in the presence or not of HLF-MBIC were removed from wells and stored at −20 °C for proteomic analysis.

The effects of HLF on bacterial motility were also determined in Petri dishes (polystyrene, diameter of 50 mm) containing 10 mL of LB added with increasing HLF concentrations, as above described.

2.4. GeLC-MS/MS analysis of proteins from planktonic cells

Proteome changes were determined in planktonic cells grown in 6 wells polystyrene microplates containing 5 mL of LB added or not with HLF-MBIC for 48 h at 15 and 30 °C. Three biological replicates for each sample were performed. After incubation planktonic cells were harvested by centrifugation at 7500 ×*g* for 10 min at 4 °C. Cell pellets were washed twice with 1 mL of TE buffer (10 mM Tris, 1 mM EDTA, pH 8.0), and re-suspended in 700 µL of TE buffer containing 1% Triton X-100 (v/v; Sigma-Aldrich, Milan, Italy). Cell suspension was then transferred in a 2 mL screw cap micro tube containing 500 µL of glass beads with a

diameter of 0.1 mm (Sigma-Aldrich). Mechanical disruption of the cells was achieved using a FastPrep®-24 homogenizer (MP Biomedicals Life Sciences) for 30 s at 6.5 m/s (3 cycles). Cell debris and glass beads were separated from the proteins by two centrifugation-steps (20,600 ×*g*, 30 min at 4 °C). Soluble proteins were then precipitated overnight at −20 °C by adding 6 vol of ice-cold acetone, and re-suspended in 8 M urea/2 M thiourea buffer. After measuring protein concentration by Roti-Nanoquant (Carl Roth, GmbH, Germany), 25 µg of proteins from each sample were separated by 1D-SDS-PAGE using Criterion TGX Precast Gels (BioRad Laboratories, Hercules, CA, USA) for 1 h at 150 V. Each lane was cut in ten equidistant pieces and these were subsequently subjected to trypsin in-gel digestion as described by Grube et al. (2015). The peptide mixtures were desalted by Zip-Tip µC18 pipette tips (Millipore, USA).

LC-MS/MS analyses were done using an EASY-nLC coupled to a LTQ Orbitrap Velos mass spectrometer (Thermo Fisher Scientific, Waltham, USA). Peptide mixtures were separated by Reverse Phase (RP) chromatography with a non-linear 75 min gradient from 5 to 75% buffer (0.1% acetic acid in acetonitrile) and a flow rate of 300 nL/min. All samples were measured in parallel mode. Survey scans were recorded in the Orbitrap with a resolution of 30,000 in a m/z range from 300 to 2000. The 20 most intense peaks were selected for collision-induced fragmentation in the LTQ, excluding ions with unknown charge state and singly-charged ions. Dynamic exclusion of precursor ions was enabled after 20 s. Internal calibration was used (lock-mass 445,120025).

2.5. Protein identification

For protein identification, spectra were searched against the annotated protein sequences from the respective *P. fluorescens* ITEM 17298 genome (Fanelli et al., 2017), including reverse sequences and common laboratory contaminants (11,526 entries). Database searches were performed using Sorcerer SEQUEST (Lundgren et al., 2009; Version v. 27 rev. 11, Thermo Scientific) and Scaffold 4.0.5 (Proteome Software, Portland, OR, USA) with the following search parameters: parent ion tolerance: 10 ppm, up to two missed cleavages were allowed and methionine was set as variable modification (López-Mondéjar et al., 2016). Protein quantification was based on the normalized spectrum abundance factor (NSAF; Zybailov et al., 2006). Functional classification of proteins was done using Prophane 2.0 (www.prophane.de) and is based on TIGRFAMs annotations. Voronoi treemaps were generated using Paver (Decodon, Greifswald, Germany; http://www.decodon.com/). An analysis of KEGG pathways was also carried out; KO identifiers were extrapolated by Uniprot database through Uniprot accession numbers available in genome file.

The raw mass spectrometry data have been deposited to the ProteomeXchange Consortium (http://proteomecentral.proteomexchange.org) via the PRIDE partner repository (Vizcaíno et al., 2016) with the dataset identifier PXD010477 (user: reviewer49185@ebi.ac.uk,password: hnkNIhfw).

2.6. Experimental design and statistical rationale

All experiments were conducted in three independent biological replicates; only static biofilm assay was performed with 8 biological replicates. Homegeneity of variances was assessed by Levene's test ($P < 0.05$) before conducting a two-way ANOVA with SPSS 20.0 (IBM, Armonk, NY, USA) to examine the effects of time, temperature levels on planktonic cell optical density, related biofilm biomass, and colony diameters in swarming and swimming assays. The two-way ANOVA was also carried out in order to examine the effects of the sub-lethal HLF concentrations on *P. fluorescens* ITEM 17298 counts and biofilm biomass in relation to incubation time at each incubation temperature. Multicomparison analyses were performed by Tukey's HSD post hoc-test ($P < 0.05$) in order to evaluate differences among the means of each assay.

Proteins detected in two out of three biological replicates were considered for statistical analysis using MeV v4.8.1 (Saeed et al., 2003). Each group of samples was compared by Student's t-test with a *P*-value of 0.01. Only proteins showing at least 2 fold changes in addition to statistical significance were considered for further analysis. So-called 'off/on' proteins needed to be detected or absent in at least two replicates of one experimental condition.

3. Results

3.1. Genomic features of P. fluorescens ITEM 17298

The draft genome sequencing resulted in 18 MB of 125 bp paired-end reads and indicated a genomic size of 6,318,747 bp with a GC content of 59%. The evaluation of the raw data quality performed by FastQC software indicated that more that 95% of reads per sample showed an average quality score higher than 30. Reads were assembled into 247 contigs > 200 bp (Fanelli et al., 2017). Analysis of protein domains categorized 48 of the predicted proteins as involved in antibiotic and cationic antimicrobial peptides resistance, 176 in biosynthesis of antibiotics, 4 in putrescine biosynthesis and 56 in virulence.

3.2. Phenotypic changes of P. fluorescens ITEM 17298 in response to the temperature

In the first 24 h of incubation, the growth of *P. fluorescens* was lower at 15 °C than at 30 °C (absorbance values OD_{600nm} of 0.44 ± 0.008 and 1.16 ± 0.12, respectively). This difference was leveled out after additional 24 h of incubation (1.9 ± 0.05 and 1.7 ± 0.14, respectively). By contrast, at both sampling times, biofilm biomass registered at 15 °C was higher than that determined at 30 °C (Fig. 1). Two-way ANOVA confirmed the statistically significant interaction between the effects of time and temperature on biofilm formation (F (2, 30) = 17.420, $p = 9.531 \times 10^{-6}$). Simple main effects analysis showed that at 15 °C the biofilm yields were significantly ($p < 0.000002$) higher than those shown at 30 °C throughout the entire incubation period.

At both incubation temperatures *P. fluorescens* was able to undertake all three types of motility (Fig. 2).

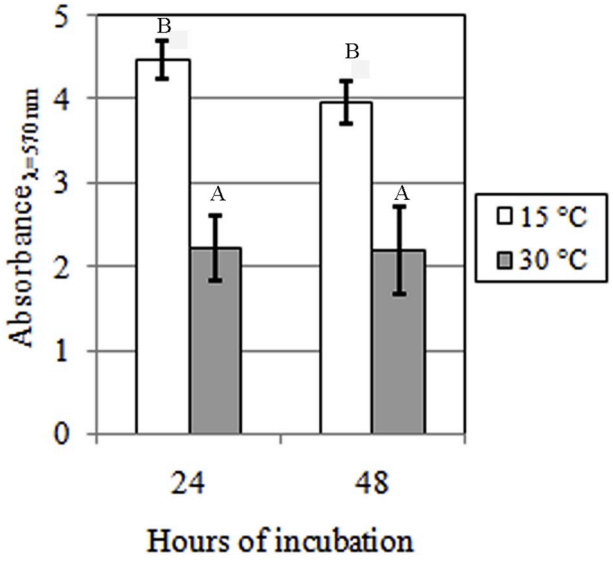

Fig. 1. Biofilm biomass produced by *P. fluorescens* ITEM 17298, grown at two temperatures (15 °C and 30 °C) measured at 24 and 48 h. Values were determined by measuring the absorbance of crystal violet (CV) at 570 nm (O'Toole, 2011). Bars represent the average ± the standard deviation (n = 8). Similar values ($P > 0.05$) of CV are annoted with the same superscript letters according to *post hoc* HSD Tukey's test.

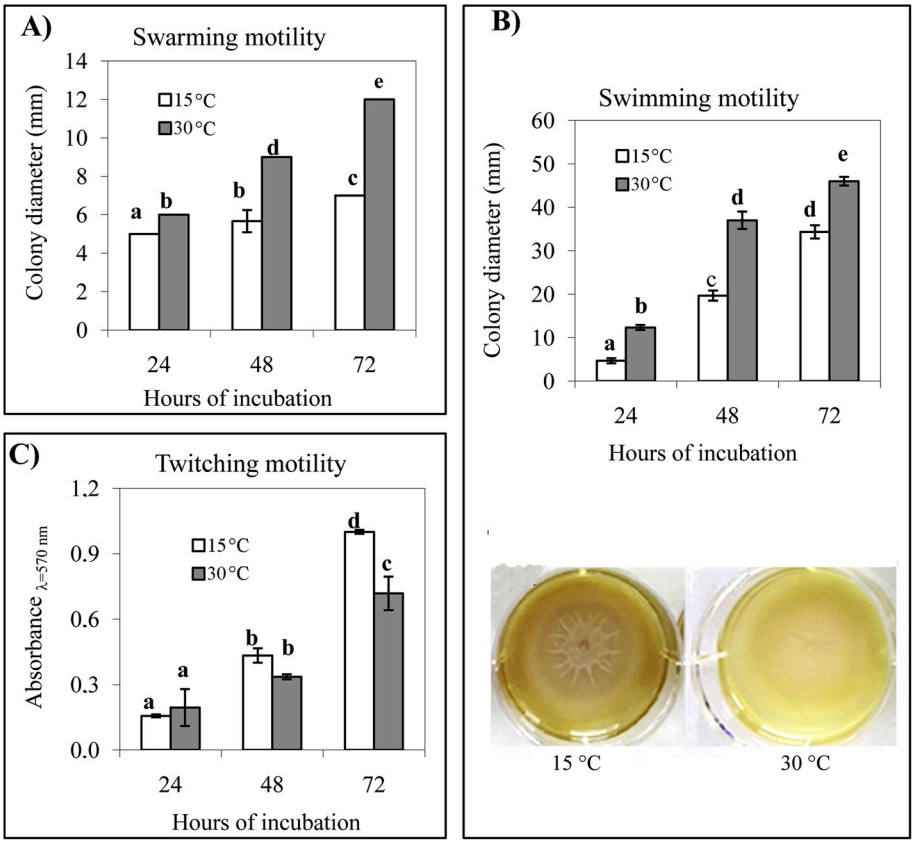

Fig. 2. Motility assays performed at 15 and 30 °C for 72 h. Swarming (**A**) and swimming motility (**B**) of *P. fluorescens* ITEM 17298 in LB agar. Values represent the mean diameter of corresponding motility zones. Twitching motility (**C**) of *P. fluorescens* ITEM 17298 in LB; these values were determined by measuring the absorbance of crystal violet (CV) at 570 nm. Bars represent the average ± the standard deviation (n = 3). Similar values ($P > 0.05$) for each motility parameter are annoted with the same superscript letters according to HSD Tukey's test. (For interpretation of the references to color in this figure legend, the reader is referred to the Web version of this article.)

The results showed a statistically significant ($P < 0.05$) interaction between experimental parameters (temperature and time of incubation) on the analyzed variable. Simple main effects analysis showed that the values of swarming and swimming motility of the strain grown at 30 °C were significantly higher than those found at 15 °C ($p < 2.2 \times 10^{-4}$) at each analyzed time point. A time-dependent increase was also found for both parameters (Fig. 2A and B).

However, the swimming assay performed at 15 °C showed that the strain formed tendrils migrating outwards from the point of bacterial inoculation, with continued branching as the bacteria moved farther from the center (Fig. 2B). As concerns twitching motility, significant differences in biofilm biomass quantified at the bottom of the plate, were registered at 72 h of incubation; at this time of sampling, the absorbance values showed increased twitching motility at 15 °C (Fig. 2C).

3.3. Evaluation of the HLF treatment: MBIC determination and motility assay

In order to establish the lowest amount able to inhibit biofilm formation without affecting bacterial growth, HLF was preliminarily assayed at different concentrations by monitoring *P. fluorescens* ITEM 17298 counts at both experimental temperatures. The results showed that no growth was registered using 12 mg/mL of HLF; by contrast, a significant ($p = 1.109 \times 10^{-7}$) reduction in cell counts by average of 3 log CFU/mL was observed in cultures treated with 6 mg/mL of HLF compared to the untreated control sample at each experimental temperature throughout the incubation period (data not shown). In addition, and concerning the two lowest HLF concentrations (1.5 and 3 mg/mL) together with the untreated control sample, two-way ANOVA results revealed that the growth of the tested strain at each incubation temperature was statistically affected only by time ($P < 0.05$) up to 24 h regardless the applied HLF concentrations (Fig. S1). In fact, no significant differences ($P > 0.0.5$) were found among treated and control samples at each incubation time suggesting that HLF concentrations lesser or equal than 3 mg/mL did not counteract the growth of the strain (Fig. S1). These concentrations were thus selected to perform the subsequent biofilm inhibition assay.

Results from biofilm biomass determination showed that the HLF concentration of 3 mg/mL was able to reduce the biofilm biomass by an average of *ca.* 74% and 54% at 15 and 30 °C, respectively, over the entire period of incubation (Fig. 3). By contrast, the lowest HLF concentration (1.5 mg/mL) led to a slight reduction (*ca.* 25%, on average). Based on these results HLF-MBIC value was established at 3 mg/mL.

HLF concentrations (ranging from 12 to 1.5 mg/mL) were also

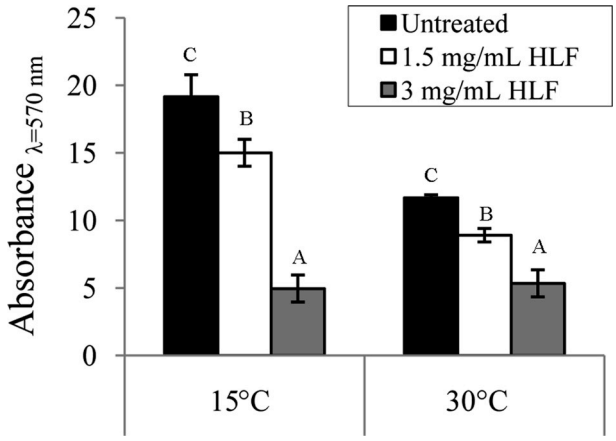

Fig. 3. Biofilm biomass produced by *P. fluorescens* ITEM 17298 treated with 1.5 and 3 mg/mL of HLF at 15 °C and 30 °C for 48 h. Values were determined by measuring the absorbance of crystal violet at 570 nm. Bars represent the average ± the standard deviation (n = 3). Different superscript letters represent values statistically different ($P < 0.05$) within the same incubation temperature and according to HSD Tukey's test.

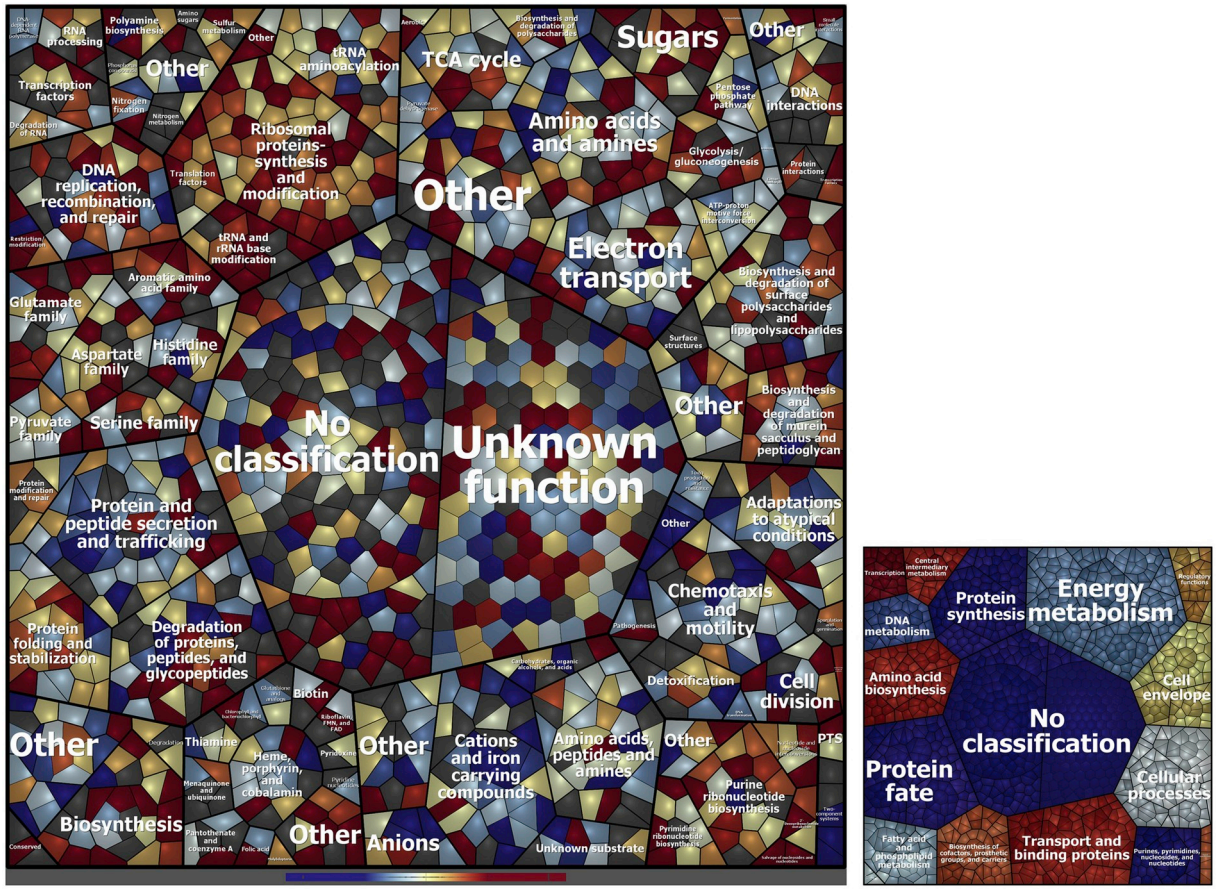

Fig. 4. Voronoi treemap visualization of *P. fluorescens* ITEM 17298 protein pattern cultivated in LB medium at 15 °C and 30 °C. Proteins are depicted as single cells and grouped according to their functional classification. Classification was achieved using *Prophane 2.0* software and is based on TIGRFAMs. Large treemap: Proteins with higher amounts at 30 °C are shown in blue; proteins with higher amounts at 15 °C are shown in red. Grey cells represent proteins that were not identified in the respective condition. Small treemap represents higher level of functional classification (main role), whereas large treemap shows subrole level. (For interpretation of the references to color in this figure legend, the reader is referred to the Web version of this article.)

tested in motility assays at both temperatures. The treatment with 12 mg/mL caused a reduction of colony diameter in swarming motility at both temperatures (Fig. S2, panel A); similar results were registered also in twitching assay (Fig. S2, panel C). By contrast, in swimming motility the supplementation of HLF caused significant differences only at 15 °C; indeed, under this temperature of incubation, a significant reduction of colony diameter was registered for the culture incubated in the presence of 12 mg/mL.HLF concentrations of 3 mg/mL inhibited tendrils development for 48 h; this effect persisted for 72 h with 6 mg/mL of HLF (Fig. S2, panel B). No changes were instead registered for the lowest HLF concentration (1.5 mg/mL; Fig. S2, panel B).

3.4. Effect of incubation temperature on the proteome of P. fluorescens ITEM 17298 planktonic cells in the absence of HLF

The comparative proteomic analyses of cell cultures, grown at 15 and 30 °C, allowed to identify 1143 proteins in at least two biological replicates (Fig. 4, Supplementary Table S1). Among these, 871 proteins were identified in both growth conditions; 186 were exclusively induced at 15 °C, whilst 86 were found only at 30 °C. Moreover, based on normalized spectral counts 298 proteins were found to be differentially expressed ($P < 0.01$, at least two-fold change).

As shown in Fig. 4 and Supplementary S3, proteins of all functional classes altered their amount at 15 °C in comparison to 30 °C. In order to decipher main differences, a deep analysis of metabolic pathways complemented by genome sequencing were performed.

Genomic analysis showed that 6-phosphofructokinase was absent in *P. fluorescens* ITEM 17298; thus, it could be supposed that glucose was metabolized through the Entner-Doudoroff pathway. Moreover, at 15 °C the levels of the enzymes involved in this metabolic pathway (PROKKA_04144 and PROKKA_05654) clearly increased; high amounts of enzymes correlated to ribose metabolism and pentose phosphate pathway (PROKKA_03487, PROKKA_01588, PROKKA_02784) and releasing glyceraldehyde-3-phosphate (G3P) intermediate were also found; then, G3P was converted into pyruvate by the 15°C-induced PROKKA_02238, PROKKA_04749, PROKKA_04632, PROKKA_02035, and PROKKA_02420 (Tables 1 and 2).

The pyruvate produced was putatively metabolized both for amino acids (valine and leucine, through the up-regulated PROKKA_05528 and PROKKA_05530) and fatty acid biosynthesis, also strongly stimulated at 15 °C (Fig. 4, Supplementary Table S1).

As regards amino acid metabolism, at 15 °C increased concentrations were observed for enzymes involved in tryptophan and tyrosine (*via* shikimate pathway), serine, glutamate and aspartate biosynthesis (Fig. 4, Table 1 and Supplementary S1). In addition, glutamate was also generated both by the proline oxidation (PROKKA_03112) and from oxoglutarate (PROKKA_01879), in turn released from enzymes (PROKKA_02649; PROKKA_03275, PROKKA_02416 and PROKKA_04321, Table 1) involved in the synthesis of polyamines (putrescine and spermidine).

Signal transduction pathways, regulatory functions as well as transcriptional processes also changed indicating adaptation processes to different temperatures (Fig. 4 and Supplementary S3, and Table S1). Among regulators, positively affected by the low temperature, we found

Table 1
Proteins induced at 15 °C in comparison to 30 °C.

Identifier	Function[a]	Fold change[b] 15°C/30°C
Amino acid biosynthesis		
PROKKA_00444	Pyrroline-5-carboxylate reductase	on
PROKKA_00484	5,10-methylenetetrahydrofolate reductase	on
PROKKA_01073	Histidinol-phosphate aminotransferase	on
PROKKA_02680	D-lactate dehydrogenase	on
PROKKA_02989	1-(5-phosphoribosyl)-5-[(5-phosphoribosylamino)methylideneamino] imidazole-4-carboxamide isomerase	on
PROKKA_03376	Diaminopimelate epimerase	on
PROKKA_03460	Gamma-glutamylputrescine synthetase PuuA	on
PROKKA_03906	Phospho-2-dehydro-3-deoxyheptonate aldolase	on
PROKKA_03985	3-phosphoshikimate 1-carboxyvinyltransferase	on
PROKKA_04062	2-hydroxy-3-keto-5-methylthiopentenyl-1-phosphate phosphatase	on
PROKKA_04321	Carboxynorspermidine synthase	on
PROKKA_04397	Shikimate 5-dehydrogenase-like protein	on
PROKKA_05528	3-isopropylmalate dehydratase small subunit 1	on
PROKKA_05530	3-isopropylmalate dehydrogenase	on
PROKKA_04034	Argininosuccinate synthase	10.90
PROKKA_04490	Phosphoserine aminotransferase	7.72
PROKKA_00579	Tryptophan synthase alpha chain	4.27
PROKKA_01890	Aspartokinase	4.22
PROKKA_04932	Glutamate 5-kinase	3.63
PROKKA_05654	2-dehydro-3-deoxy-phosphogluconate aldolase	3.12
PROKKA_04081	Glutamate synthase [NADPH] large chain	3.00
PROKKA_04990	Homoserine dehydrogenase	2.98
PROKKA_05356	Phospho-2-dehydro-3-deoxyheptonate aldolase, Tyr-sensitive	2.70
PROKKA_03160	Phosphoserine phosphatase	2.63
PROKKA_00905	Tryptophan synthase alpha chain	2.43
PROKKA_04707	Anthranilate synthase component 1	2.11
Biosynthesis of cofactors, prosthetic groups, and carriers		
PROKKA_00136	ATPase family associated with various cellular activities (AAA)	on
PROKKA_00405	Dihydrofolate reductase type 3	on
PROKKA_01482	NifU-like protein	on
PROKKA_01888	Low specificity L-threonine aldolase	on
PROKKA_02355	tRNA-modifying protein YgfZ	on
PROKKA_02541	Bifunctional protein FolD protein	on
PROKKA_03079	Uroporphyrinogen decarboxylase	on
PROKKA_03546	Riboflavin biosynthesis protein RibBA	on
PROKKA_03551	GTP cyclohydrolase-2	on
PROKKA_03555	1-deoxy-D-xylulose-5-phosphate synthase	on
PROKKA_03878	4-hydroxy-3-methylbut-2-enyl diphosphate reductase	on
PROKKA_04184	Sulfite reductase [ferredoxin]	on
PROKKA_04334	DNA nickase	on
PROKKA_00427	Protease 3 precursor	9.68
PROKKA_03618	Glutamate-1-semialdehyde 2,1-aminomutase	5.13
PROKKA_00418	Phosphopantetheine adenylyltransferase	4.41
PROKKA_01483	Cysteine desulfurase	2.65
PROKKA_03437	2-octaprenylphenol hydroxylase	2.19
PROKKA_04743	2-C-methyl-D-erythritol 2,4-cyclodiphosphate synthase	2.02
Cell envelope		
PROKKA_01070	UDP-N-acetylglucosamine 1-carboxyvinyltransferase	on
PROKKA_01121	D-alanine–D-alanine ligase	on
PROKKA_01908	Membrane bound L-sorbosone dehydrogenase	on
PROKKA_03735	Phosphoglucosamine mutase	on
PROKKA_04504	UDP-glucose 4-epimerase	on
PROKKA_04558	Poly-beta-1,6-N-acetyl-D-glucosamine N-deacetylase precursor	on
PROKKA_04759	UDP-3-O-acylglucosamine N-acyltransferase	on
PROKKA_04779	Cellulose synthase 1	on
PROKKA_01120	UDP-N-acetylmuramate–L-alanine ligase	13.04
PROKKA_02849	Glucose-1-phosphate thymidylyltransferase 2	5.84
PROKKA_01125	UDP-3-O-[3-hydroxymyristoyl] N-acetylglucosamine deacetylase	5.39
PROKKA_03355	Alanine racemase	5.34
PROKKA_03138	Bifunctional protein HldE	4.69
PROKKA_01039	Rod shape-determining protein MreB	3.34
PROKKA_02911	D-methionine-binding lipoprotein MetQ precursor	3.12
PROKKA_01060	Lipopolysaccharide export system protein LptA precursor	2.82
PROKKA_02851	dTDP-4-dehydrorhamnose reductase	2.69
PROKKA_00635	Glutamine–fructose-6-phosphate aminotransferase [isomerizing]	2.28
PROKKA_02850	dTDP-4-dehydrorhamnose 3,5-epimerase	2.27
PROKKA_03604	Membrane-bound lytic murein transglycosylase B precursor	2.17
PROKKA_01117	UDP-N-acetylmuramoylalanine–D-glutamate ligase	2.12
PROKKA_03033	Glucans biosynthesis protein G precursor	2.05
PROKKA_01062	3-deoxy-D-manno-octulosonate 8-phosphate phosphatase KdsC	2.04
Cellular processes		
PROKKA_01123	Cell division protein FtsA	on
PROKKA_01309	General stress protein 14	on
PROKKA_01755	Flagellar motor switch protein FliN	on
PROKKA_02616	NADP-dependent glyceraldehyde-3-phosphate dehydrogenase	on
PROKKA_03063	cell division protein FtsN	on
PROKKA_03674	Catalase precursor	on
PROKKA_04028	Septum site-determining protein MinD	on
PROKKA_04126	Septum site-determining protein MinD	on
PROKKA_04934	Hydroperoxy fatty acid reductase gpx2	on
PROKKA_01124	Cell division protein FtsZ	6.09
PROKKA_03612	Magnesium and cobalt efflux protein CorC	4.78
PROKKA_01272	Chitinase D precursor	4.58
PROKKA_03681	Serine hydroxymethyltransferase 2	3.05
PROKKA_05169	Alkyl hydroperoxide reductase subunit C	2.43
PROKKA_03387	Sensory transduction protein LytR	2.02
Central intermediary metabolism		
PROKKA_02416	S-adenosylmethionine synthase	on
PROKKA_02855	3′(2′),5′-bisphosphate nucleotidase CysQ	on
PROKKA_03275	Biosynthetic arginine decarboxylase	on
PROKKA_05514	(R)-stereoselective amidase	on
PROKKA_04344	Peptidyl-prolyl cis-trans isomerase C	4.40
PROKKA_04698	Chaperone SurA precursor	2.24
DNA metabolism		
PROKKA_01794	ATP-dependent DNA helicase RecQ	on
PROKKA_03707	Type I restriction enzyme EcoKI M protein	on
PROKKA_04026	DNA mismatch repair protein MutS	on
PROKKA_04576	Type I restriction enzyme EcoR124II R protein	on
PROKKA_04579	putative type I restriction enzymeP M protein	on
PROKKA_05553	8-oxo-dGTP diphosphatase	on
PROKKA_00259	Recombination-associated protein RdgC	3.39
PROKKA_00612	DNA polymerase III subunit beta	3.20
PROKKA_03903	ATP-dependent RNA helicase DeaD	2.85
PROKKA_04737	Cold shock protein CapB	2.81
PROKKA_01628	DNA-binding protein HRm	2.70
PROKKA_00481	ATP-dependent RNA helicase RhlE	2.43
PROKKA_04882	recombinase A	2.37
PROKKA_02589	Exodeoxyribonuclease III	2.33
PROKKA_00610	DNA gyrase subunit B	2.06
Energy metabolism		
PROKKA_00293	3-oxoadipate enol-lactonase 2	on
PROKKA_00606	D-glycero-beta-D-manno-heptose-1,7-bisphosphate 7-phosphatase	on
PROKKA_00980	Tagatose-6-phosphate kinase	on
PROKKA_01297	Fructose dehydrogenase large subunit	on
PROKKA_01306	NADH oxidase	on
PROKKA_01396	Levansucrase	on
PROKKA_01588	Transketolase	on
PROKKA_01831	8-oxoguanine deaminase	on
PROKKA_01879	Succinylornithine transaminase/acetylornithine aminotransferase	on
PROKKA_01882	Arginine N-succinyltransferase subunit beta	on
PROKKA_02631	NADH-quinone oxidoreductase subunit I	on
PROKKA_02783	D-ribose pyranase	on

(*continued on next page*)

Table 1 (*continued*)

Identifier	Function[a]	Fold change[b] 15°C/30°C
PROKKA_02784	Ribokinase	on
PROKKA_02793	hypothetical protein	on
PROKKA_03016	8-oxoguanine deaminase	on
PROKKA_03017	HTH-type transcriptional repressor YvoA	on
PROKKA_03440	Aminomethyltransferase	on
PROKKA_03487	Ribose-5-phosphate isomerase A	on
PROKKA_03492	Phosphoenolpyruvate-protein phosphotransferase	on
PROKKA_03672	Ferredoxin–NADP reductase	on
PROKKA_04041	Glutaredoxin-4	on
PROKKA_04187	Pyruvate dehydrogenase [ubiquinone]	on
PROKKA_04385	Disulfide-bond oxidoreductase YfcG	on
PROKKA_04900	Tryptophan 2,3-dioxygenase	on
PROKKA_04909	Catechol 1,2-dioxygenase	on
PROKKA_04958	Trehalose-6-phosphate hydrolase	on
PROKKA_04960	Phosphoenolpyruvate-protein phosphotransferase	on
PROKKA_05120	hypothetical protein	on
PROKKA_02420	Phosphoglycerate kinase	12.53
PROKKA_02649	Isocitrate dehydrogenase [NADP]	7.27
PROKKA_02092	Electron transfer flavoprotein subunit alpha	6.46
PROKKA_02093	Electron transfer flavoprotein subunit beta	5.29
PROKKA_02634	NADH-quinone oxidoreductase subunit F	4.50
PROKKA_02836	UDP-glucose 4-epimerase	4.17
PROKKA_05658	(R)-specific enoyl-CoA hydratase	4.01
PROKKA_02035	Phosphoenolpyruvate synthase	3.78
PROKKA_03112	Bifunctional protein PutA	3.55
PROKKA_04632	Pyruvate kinase II	3.48
PROKKA_02633	NADH-quinone oxidoreductase subunit G	3.40
PROKKA_05607	Carbamate kinase 2	3.28
PROKKA_02423	Fructose-bisphosphate aldolase	3.23
PROKKA_01450	Non-heme chloroperoxidase	3.05
PROKKA_04938	Glucosaminate ammonia-lyase	2.88
PROKKA_01079	Malate:quinone oxidoreductase	2.54
PROKKA_04460	Malate:quinone oxidoreductase	2.51
PROKKA_04749	Enolase	2.44
PROKKA_02238	Glyceraldehyde-3-phosphate dehydrogenase	2.40
PROKKA_05696	Glycerophosphoryl diester phosphodiesterase	2.29
PROKKA_02510	2-oxoisovalerate dehydrogenase subunit alpha	2.05
PROKKA_01884	N-succinylarginine dihydrolase	2.03
Fatty acid and phospholipid metabolism		
PROKKA_01305	Cyclopentanol dehydrogenase	on
PROKKA_01776	3-oxoacyl-[acyl-carrier-protein] synthase 3	on
PROKKA_01961	3-oxoacyl-[acyl-carrier-protein] synthase 3	on
PROKKA_05080	Malonyl CoA-acyl carrier protein transacylase	on
PROKKA_05542	Glucose 1-dehydrogenase 1	on
PROKKA_02045	Aconitate hydratase 1	7.64
PROKKA_00314	3-oxoacyl-[acyl-carrier-protein] synthase 1	6.39
PROKKA_05079	3-oxoacyl-[acyl-carrier-protein] reductase FabG	4.36
PROKKA_04753	Acetyl-coenzyme A carboxylase carboxyl transferase subunit alpha	4.19
PROKKA_03267	Biotin carboxylase	3.91
PROKKA_05078	Acyl carrier protein	2.58
PROKKA_00502	Acyl-CoA dehydrogenase	2.27
PROKKA_05221	Acyl-CoA dehydrogenase	2.16
No classification		
PROKKA_02270	Kinase A inhibitor	on
PROKKA_00123	hypothetical protein	on
PROKKA_00238	Protein of unknown function, DUF	on
PROKKA_00297	Putative NADP-dependent oxidoreductase YfmJ	on
PROKKA_00557	hypothetical protein	on
PROKKA_00573	Limonene 1,2-monooxygenase	on
PROKKA_00623	putative chromosome-partitioning protein ParB	on
PROKKA_00653	hypothetical protein	on
PROKKA_00705	Putative glucose-6-phosphate 1-epimerase	on
PROKKA_00846	hypothetical protein	on
PROKKA_00859	Decarbamoyl novobiocin carbamoyltransferase	on
PROKKA_00901	putative oxidoreductase YjmC	on
PROKKA_00963	hypothetical protein	on
PROKKA_01044	hypothetical protein	on
PROKKA_01047	hypothetical protein	on
PROKKA_01240	putative rhodanese-related sulfurtransferase	on

Table 1 (*continued*)

Identifier	Function[a]	Fold change[b] 15°C/30°C
PROKKA_01298	hypothetical protein	on
PROKKA_01299	hypothetical protein	on
PROKKA_01517	hypothetical protein	on
PROKKA_01700	hypothetical protein	on
PROKKA_01921	hypothetical protein	on
PROKKA_02407	hypothetical protein	on
PROKKA_02569	putative chaperone protein EcpD	on
PROKKA_02721	Gramicidin S synthase 2	on
PROKKA_02722	Tyrocidine synthase 3	on
PROKKA_02831	hypothetical protein	on
PROKKA_02980	hypothetical protein	on
PROKKA_03018	hypothetical protein	on
PROKKA_03311	PP2C-family Ser/Thr phosphatase	on
PROKKA_03324	NAD dependent epimerase/dehydratase family protein	on
PROKKA_03372	hypothetical protein	on
PROKKA_03375	hypothetical protein	on
PROKKA_03383	Phosphate-starvation-inducible E	on
PROKKA_03426	Quinone oxidoreductase 1	on
PROKKA_03433	hypothetical protein	on
PROKKA_03476	hypothetical protein	on
PROKKA_03713	hypothetical protein	on
PROKKA_03836	Ribosome-binding ATPase YchF	on
PROKKA_04331	hypothetical protein	on
PROKKA_04378	SCP-2 sterol transfer family protein	on
PROKKA_04402	putative protease YhbU precursor	on
PROKKA_04444	D-inositol-3-phosphate glycosyltransferase	on
PROKKA_04575	hypothetical protein	on
PROKKA_04639	Flavin reductase like domain protein	on
PROKKA_04700	Phosphotransferase enzyme family protein	on
PROKKA_04719	Nitronate monooxygenase	on
PROKKA_04786	hypothetical protein	on
PROKKA_04927	hypothetical protein	on
PROKKA_04989	Thiol:disulfide interchange protein DsbC precursor	on
PROKKA_05083	hypothetical protein	on
PROKKA_05381	Xylose isomerase-like TIM barrel	on
PROKKA_05473	hypothetical protein	on
PROKKA_05492	hypothetical protein	on
PROKKA_05549	AAA-like domain protein	on
PROKKA_05752	hypothetical protein	on
PROKKA_04144	6-phosphogluconolactonase	5.46
PROKKA_02387	hypothetical protein	4.25
PROKKA_01604	Quinoprotein glucose dehydrogenase	3.82
PROKKA_04468	Putative reductase/y4119/YP_4011	3.71
PROKKA_01655	hypothetical protein	3.22
PROKKA_03582	hypothetical protein	3.10
PROKKA_01238	hypothetical protein	3.00
PROKKA_01727	hypothetical protein	2.48
PROKKA_04711	Indole-3-glycerol phosphate synthase	2.44
PROKKA_00243	Carboxymuconolactone decarboxylase family protein	2.40
PROKKA_02865	Tetratricopeptide repeat protein	2.34
PROKKA_02240	hypothetical protein	2.11
PROKKA_02623	hypothetical protein	0.27
Protein fate		
PROKKA_00428	Signal recognition particle receptor FtsY	on
PROKKA_01479	Chaperone protein HscA	on
PROKKA_02233	Lipoprotein-releasing system transmembrane protein LolE	on
PROKKA_02543	ATP-dependent Clp protease proteolytic subunit	on
PROKKA_02658	Outer-membrane lipoprotein carrier protein precursor	on
PROKKA_03402	Enhancing lycopene biosynthesis protein 2	on
PROKKA_04332	General stress protein 18	on
PROKKA_05350	Lipoprotein-releasing system ATP-binding protein LolD	on
PROKKA_05353	putative L,D-transpeptidase YbiS precursor	on
PROKKA_02545	Lon protease	8.10
PROKKA_00281	Beta-Ala-Xaa dipeptidase	6.64
PROKKA_01089	Metalloprotease LoiP precursor	3.91
PROKKA_04925	FKBP-type 22 kDa peptidyl-prolyl cis-trans isomerase	3.73

(*continued on next page*)

Table 1 (*continued*)

Identifier	Function[a]	Fold change[b] 15°C/30°C
PROKKA_01048	peptidase PmbA	3.49
PROKKA_04593	Tail-specific protease precursor	3.18
PROKKA_00118	putative lipoprotein YiaD precursor	3.01
PROKKA_01952	Peptidyl-prolyl cis-trans isomerase A precursor	2.64
PROKKA_02544	ATP-dependent Clp protease ATP-binding subunit ClpX	2.21
PROKKA_03302	hypothetical protein	2.15
Protein synthesis		
PROKKA_00031	30S ribosomal protein S17	on
PROKKA_00040	50S ribosomal protein L30	on
PROKKA_00425	Ribosomal RNA small subunit methyltransferase D	on
PROKKA_00477	Ribosomal RNA small subunit methyltransferase E	on
PROKKA_00620	tRNA uridine 5-carboxymethylaminomethyl modification enzyme MnmG	on
PROKKA_01468	GTPase Der	on
PROKKA_01493	S-adenosylmethionine:tRNA ribosyltransferase-isomerase	on
PROKKA_02042	Alanine–tRNA ligase	on
PROKKA_02645	tRNA-specific 2-thiouridylase MnmA	on
PROKKA_02772	Phenylalanine–tRNA ligase alpha subunit	on
PROKKA_03142	tRNA 5-methylaminomethyl-2-thiouridine biosynthesis bifunctional protein MnmC	on
PROKKA_03188	23S rRNA (guanosine-2′-O-)-methyltransferase RlmB	on
PROKKA_03266	Ribosomal protein L11 methyltransferase	on
PROKKA_03741	tRNA pseudouridine synthase B	on
PROKKA_03845	Peptide chain release factor 1	on
PROKKA_04684	30S ribosomal protein S21	on
PROKKA_05082	50S ribosomal protein L32	on
PROKKA_04931	GTPase Obg	23.36
PROKKA_00012	50S ribosomal protein L1	15.56
PROKKA_00022	50S ribosomal protein L3	7.04
PROKKA_00036	30S ribosomal protein S8	5.94
PROKKA_00013	50S ribosomal protein L10	5.16
PROKKA_05366	Elongation factor P	4.58
PROKKA_00045	30S ribosomal protein S4	4.31
PROKKA_03838	50S ribosomal protein L25	4.21
PROKKA_03189	30S ribosomal protein S6	4.07
PROKKA_00037	50S ribosomal protein L6	4.01
PROKKA_00039	30S ribosomal protein S5	3.70
PROKKA_02661	Serine–tRNA ligase	3.37
PROKKA_00025	50S ribosomal protein L2	3.33
PROKKA_01019	50S ribosomal protein L13	3.12
PROKKA_03739	Translation initiation factor IF-2	3.02
PROKKA_02775	Translation initiation factor IF-3	2.99
PROKKA_00044	30S ribosomal protein S11	2.96
PROKKA_00033	50S ribosomal protein L24	2.82
PROKKA_01111	Ribosomal RNA small subunit methyltransferase H	2.68
PROKKA_04982	30S ribosomal protein S16	2.64
PROKKA_00011	50S ribosomal protein L11	2.35
PROKKA_04769	30S ribosomal protein S2	2.35
PROKKA_00026	30S ribosomal protein S19	2.32
PROKKA_03192	50S ribosomal protein L9	2.30
PROKKA_00041	50S ribosomal protein L15	2.28
PROKKA_01626	Valine–tRNA ligase	2.19
PROKKA_00023	50S ribosomal protein L4	2.08
PROKKA_01492	Queuine tRNA-ribosyltransferase	2.07
Purines, pyrimidines, nucleosides, and nucleotides		
PROKKA_01833	Adenine deaminase	on
PROKKA_01914	Phosphoribosylformylglycinamidine cyclo-ligase	on
PROKKA_03338	Deoxyuridine 5′-triphosphate nucleotidohydrolase	on
PROKKA_03359	Xanthine phosphoribosyltransferase	on
PROKKA_03727	Carbamoyl-phosphate synthase small chain	14.90
PROKKA_03728	Carbamoyl-phosphate synthase large chain	9.94
PROKKA_04963	Phosphoribosylformylglycinamidine synthase	6.91
PROKKA_04494	Cytidylate kinase	6.20
PROKKA_04751	CTP synthase	4.92
PROKKA_01075	Uracil phosphoribosyltransferase	4.06
PROKKA_04767	Uridylate kinase	3.27
PROKKA_00702	N5-carboxyaminoimidazole ribonucleotide synthase	3.11
PROKKA_03839	Ribose-phosphate pyrophosphokinase	3.10
PROKKA_02340	Phosphoribosylaminoimidazole-succinocarboxamide synthase	2.69
PROKKA_05100	Ribonucleoside-diphosphate reductase 1 subunit alpha	2.40
PROKKA_04977	Phosphoribosylglycinamide formyltransferase 2	2.27
PROKKA_02643	Adenylosuccinate lyase	2.26
PROKKA_03181	Adenylosuccinate synthetase	2.17
Regulatory functions		
PROKKA_00530	Response regulator PleD	on
PROKKA_01026	HTH-type transcriptional regulator LutR	on
PROKKA_03320	Hydrogen peroxide-inducible genes activator	on
PROKKA_03008	GTP-binding protein TypA/BipA	4.27
PROKKA_00527	Alginate biosynthesis transcriptional regulatory protein AlgB	2.85
PROKKA_01641	Sigma 54 modulation protein/S30EA ribosomal protein	2.60
PROKKA_02008	putative HTH-type transcriptional regulator YdfH	2.33
PROKKA_02562	putative transcriptional regulatory protein	2.31
Signal transduction		
PROKKA_01056	Nitrogen regulatory protein	on
Transcription		
PROKKA_02227	NADPH-dependent 7-cyano-7-deazaguanine reductase	on
PROKKA_03548	hypothetical protein	on
PROKKA_03419	hypothetical protein	6.72
PROKKA_03738	hypothetical protein	2.39
PROKKA_00010	hypothetical protein	2.25
Transport and binding proteins		
PROKKA_00683	Cystine-binding periplasmic protein precursor	on
PROKKA_01304	Fatty acyl-CoA reductase	on
PROKKA_01319	Hemin-binding periplasmic protein HmuT precursor	on
PROKKA_02724	Macrolide export protein MacA	on
PROKKA_03184	Iron-utilization periplasmic protein precursor	on
PROKKA_03225	Bacterioferritin	on
PROKKA_04601	Periplasmic solute binding protein family protein	on
PROKKA_05015	putative ABC transporter ATP-binding protein	on
PROKKA_04499	LPS O-antigen length regulator	4.76
PROKKA_05330	hypothetical protein	3.00
PROKKA_03683	putative ABC transporter ATP-binding protein	2.89
PROKKA_04287	Glycine betaine-binding periplasmic protein precursor	2.37

[a] Function predicted by Prokka annotation.
[b] "on " exclusively identified under 15 °C.

two members of GnrT family (PROKKA_01026 and PROKKA_02008), AlgB (PROKKA_00527), PleD (PROKKA_00530), the hydrogen peroxide-inducible genes activator (PROKKA_03320), the GTP-binding protein TypA/BipA (PROKKA_03008) involved in cold stress response. In addition, at 15 °C, we also exclusively detected the carbon storage regulator CsrA/RsmA (PROKKA_02793), implicated in changes in energy metabolism.

The level of purine and pyrimidine biosynthesis enzymes increased at 15 °C (Table 1). Likewise, protein synthesis was strongly stimulated (Fig. 4 and Fig. S2 and Table 1). However, 18 proteins involved in proteolysis also changed their levels (e.g. PROKKA_00281, PROKKA_02544, PROKKA_02545, and PROKKA_01048).

Induced proteins were also grouped in detoxification processes (PROKKA_05169) or adaptation to atypical condition, such as oxidative stress (PROKKA_03674, PROKKA_04934).

Cold stress adaptation also led to the increase of enzymes belonging

Table 2
Proteins repressed at 15 °C in comparison to 30 °C.

Identifier	Function[a]	Fold change[b] 15°C/30°C
Amino acid biosynthesis		
PROKKA_01520	Histidinol-phosphate aminotransferase 2	off
PROKKA_05541	O-succinylhomoserine sulfhydrylase	0.45
PROKKA_05608	Ornithine carbamoyltransferase, catabolic	0.44
PROKKA_01071	ATP phosphoribosyltransferase	0.44
PROKKA_00904	Tryptophan synthase beta chain	0.42
PROKKA_02986	Imidazoleglycerol-phosphate dehydratase	0.32
Biosynthesis of cofactors, prosthetic groups, and carriers		
PROKKA_03863	Ferrochelatase	off
PROKKA_03405	Delta-aminolevulinic acid dehydratase	0.48
PROKKA_04486	Ubiquinone biosynthesis O-methyltransferase	0.47
PROKKA_02094	Electron transfer flavoprotein-ubiquinone oxidoreductase	0.46
PROKKA_02662	Siroheme synthase	0.46
PROKKA_03811	Gamma-glutamyltranspeptidase precursor	0.44
Cell envelope		
PROKKA_01669	D-alanyl-D-alanine carboxypeptidase DacC precursor	off
PROKKA_04822	Glucans biosynthesis protein D precursor	0.43
PROKKA_03534	Outer membrane protein W precursor	0.32
PROKKA_02028	Outer membrane porin F precursor	0.29
PROKKA_03767	Penicillin-binding protein 1B	0.29
PROKKA_01622	Lipopolysaccharide export system permease protein LptF	0.28
PROKKA_00116	Outer membrane lipoprotein SlyB precursor	0.27
Cellular processes		
PROKKA_00520	Mce related protein	off
PROKKA_00991	Glycine betaine/carnitine/choline-binding protein OpuCC precursor	off
PROKKA_01099	Paraquat-inducible protein B	off
PROKKA_01211	Copper-transporting P-type ATPase	off
PROKKA_01766	Flagellar M-ring protein	off
PROKKA_02002	Chromosome partition protein Smc	off
PROKKA_03354	2-aminomuconate deaminase	off
PROKKA_04562	Filamentous hemagglutinin	off
PROKKA_00072	putative efflux pump membrane transporter TtgB	0.46
PROKKA_00073	putative efflux pump outer membrane protein TtgC precursor	0.45
PROKKA_01105	Osmotically-inducible protein Y precursor	0.44
PROKKA_01773	Flagellar hook-associated protein 2	0.43
PROKKA_03782	Paraquat-inducible protein B	0.38
PROKKA_05563	DNA protection during starvation protein 2	0.33
PROKKA_01775	B-type flagellin	0.32
PROKKA_00253	Heat-inducible protein	0.31
PROKKA_05581	Filamentous hemagglutinin	0.25
PROKKA_04405	Methyl-accepting chemotaxis protein PctC	0.24
PROKKA_05548	Methyl-accepting chemotaxis protein PctA	0.20
PROKKA_03040	Methyl-accepting chemotaxis protein McpS	0.20
Central intermediary metabolism		
PROKKA_00421	Coniferyl aldehyde dehydrogenase	off
PROKKA_01466	(R)-stereoselective amidase	off
PROKKA_01967	Aerotaxis receptor	0.35
DNA metabolism		
PROKKA_00722	DNA-binding protein HU-beta	off
PROKKA_02651	Cold shock-like protein CspD	off
PROKKA_03709	Type-1 restriction enzyme R protein	off
PROKKA_05569	Holliday junction ATP-dependent DNA helicase RuvA	off
PROKKA_03154	DNA topoisomerase 4 subunit B	0.46
PROKKA_04489	DNA gyrase subunit A	0.42
PROKKA_03156	DNA topoisomerase 4 subunit A	0.30
Energy metabolism		
PROKKA_00350	2-hydroxy-3-oxopropionate reductase	off
PROKKA_01785	Phenylalanine-4-hydroxylase	off
PROKKA_01980	Ubp3 associated protein Bre5	off
PROKKA_02062	Phosphorylated carbohydrates phosphatase	off
PROKKA_02464	Anthranilate 1,2-dioxygenase large subunit	off
PROKKA_02627	NADH-quinone oxidoreductase subunit M	off
PROKKA_02727	Methionine gamma-lyase	off
PROKKA_03974	Trehalose synthase/amylase TreS	off
PROKKA_04974	2,3,4,5-tetrahydropyridine-2,6-dicarboxylate N-acetyltransferase	off
PROKKA_05460	Aminomethyltransferase	off
PROKKA_01971	Cytochrome C oxidase, mono-heme subunit/ FixO	0.50
PROKKA_05189	L-glyceraldehyde 3-phosphate reductase	0.50
PROKKA_01176	Methylmalonate-semialdehyde dehydrogenase [acylating]	0.45
PROKKA_01021	Ubiquinol-cytochrome c reductase iron-sulfur subunit	0.44
PROKKA_01023	Cytochrome b/c1	0.43
PROKKA_00630	ATP synthase gamma chain	0.42
PROKKA_02507	Dihydrolipoyl dehydrogenase	0.42
PROKKA_00337	Citrate synthase	0.39
PROKKA_00360	Cytochrome c-type biogenesis protein CcmH precursor	0.38
PROKKA_01973	Cbb3-type cytochrome c oxidase subunit CcoP1	0.37
PROKKA_05220	putative enoyl-CoA hydratase echA8	0.36
PROKKA_03975	1,4-alpha-glucan branching enzyme GlgB	0.35
PROKKA_02639	Isocitrate lyase	0.35
PROKKA_01666	Ureidoglycolate lyase	0.33
PROKKA_05652	Glucose-6-phosphate 1-dehydrogenase	0.29
PROKKA_01667	Homogentisate 1,2-dioxygenase	0.25
PROKKA_01972	Cbb3-type cytochrome oxidase component FixQ	0.22
PROKKA_01022	Cytochrome b	0.17
Fatty acid and phospholipid metabolism		
PROKKA_01388	Glucose 1-dehydrogenase 1	off
PROKKA_01846	3-ketoacyl-CoA thiolase	off
PROKKA_02583	Long-chain-fatty-acid–CoA ligase	off
PROKKA_03054	Poly(hydroxyalcanoate) granule associated protein (phasin)	off
PROKKA_03347	putative cardiolipin synthase YwiE	off
PROKKA_01444	Acetyl-CoA acetyltransferase	0.49
PROKKA_01847	3-oxoacyl-[acyl-carrier-protein] reductase FabG	0.49
PROKKA_01803	Putative outer membrane protein precursor	0.35
PROKKA_02046	2-methylcitrate synthase	0.32
PROKKA_05504	Acyl-CoA dehydrogenase	0.32
PROKKA_00270	Acyl-coenzyme A dehydrogenase	0.26
No classification		
PROKKA_00089	Low-affinity inorganic phosphate transporter 1	off
PROKKA_00582	D-galactonate dehydratase	off
PROKKA_01488	hypothetical protein	off
PROKKA_01798	DNA recombination protein RmuC	off
PROKKA_02422	lysozyme inhibitor	off
PROKKA_02678	META domain protein	off
PROKKA_02708	hypothetical protein	off
PROKKA_02806	Gamma-glutamylputrescine oxidoreductase	off
PROKKA_03014	hypothetical protein	off
PROKKA_03106	Mechanosensitive channel MscK precursor	off
PROKKA_03158	hypothetical protein	off
PROKKA_03231	E3 ubiquitin-protein ligase ipaH3	off
PROKKA_03294	putative deoxyribonuclease RhsA	off
PROKKA_03473	Acyl-homoserine lactone acylase QuiP precursor	off
PROKKA_03583	Peptidase C13 family protein	off
PROKKA_03650	hypothetical protein	off
PROKKA_03686	hypothetical protein	off
PROKKA_03994	hypothetical protein	off
PROKKA_04403	Methyl-accepting chemotaxis protein PctB	off
PROKKA_04561	Hemolysin transporter protein ShlB precursor	off
PROKKA_04806	hypothetical protein	off
PROKKA_04808	hypothetical protein	off
PROKKA_04959	Maltoporin precursor	off
PROKKA_05161	hypothetical protein	off
PROKKA_05230	putative 4-deoxy-4-formamido-L-arabinose-phosphoundecaprenol deformylase ArnD	off
PROKKA_05325	General stress protein 69	off
PROKKA_05560	HIT domain protein	off

(*continued on next page*)

Table 2 (*continued*)

Identifier	Function[a]	Fold change[b] 15°C/30°C
PROKKA_03698	hypothetical protein	0.49
PROKKA_00381	hypothetical protein	0.49
PROKKA_05649	Porin B precursor	0.48
PROKKA_03317	hypothetical protein	0.48
PROKKA_00323	hypothetical protein	0.48
PROKKA_03224	putative assembly protein	0.48
PROKKA_04269	hypothetical protein	0.47
PROKKA_00112	hypothetical protein	0.47
PROKKA_04341	hypothetical protein	0.47
PROKKA_03542	hypothetical protein	0.47
PROKKA_00138	NAD-specific glutamate dehydrogenase	0.46
PROKKA_04556	hypothetical protein	0.45
PROKKA_04669	hypothetical protein	0.44
PROKKA_03678	Inner membrane protein YjiY	0.43
PROKKA_00373	putative lipoprotein YgdR precursor	0.41
PROKKA_01012	hypothetical protein	0.41
PROKKA_03272	hypothetical protein	0.41
PROKKA_03325	hypothetical protein	0.40
PROKKA_00542	hypothetical protein	0.39
PROKKA_02030	hypothetical protein	0.38
PROKKA_04259	hypothetical protein	0.38
PROKKA_01066	putative phospholipid ABC transporter-binding protein MlaD	0.36
PROKKA_05259	hypothetical protein	0.36
PROKKA_02996	molybdopterin biosynthesis protein MoeB	0.32
PROKKA_03278	hypothetical protein	0.30
PROKKA_00547	hypothetical protein	0.28
PROKKA_01962	ATP-dependent RNA helicase HrpB	0.27
PROKKA_03134	Putative glycosyltransferase EpsF	0.27
PROKKA_03149	hypothetical protein	0.27
PROKKA_03572	Inner membrane protein YghB	0.25
PROKKA_04656	Imelysin	0.24
PROKKA_03843	bacteriophage N4 receptor, outer membrane subunit	0.21
PROKKA_01609	Chagasin family peptidase inhibitor I42	0.17
Protein fate		
PROKKA_00361	Thiol:disulfide interchange protein DsbE	off
PROKKA_00681	Extracellular serine protease precursor	off
PROKKA_01742	Chemotaxis protein CheA	off
PROKKA_03062	ATP-dependent protease subunit HslV	off
PROKKA_03165	Motility protein B	off
PROKKA_03297	Chaperone protein ClpB	off
PROKKA_02089	putative lipoprotein YiaD precursor	0.50
PROKKA_01619	Signal peptidase I	0.50
PROKKA_04665	60 kDa chaperonin	0.50
PROKKA_01469	Outer membrane protein assembly factor BamB precursor	0.49
PROKKA_01103	putative lipoprotein YiaD precursor	0.47
PROKKA_01205	Peptidoglycan-binding protein ArfA	0.47
PROKKA_01608	Lon protease	0.46
PROKKA_05085	Putative signal peptide peptidase SppA	0.45
PROKKA_05384	Carboxypeptidase G2 precursor	0.44
PROKKA_03307	hypothetical protein	0.43
PROKKA_04761	Outer membrane protein assembly factor BamA precursor	0.40
PROKKA_04617	Aminopeptidase	0.39
PROKKA_02677	Thiol-disulfide oxidoreductase ResA	0.37
PROKKA_03179	Modulator of FtsH protease HflC	0.37
PROKKA_01491	preprotein translocase subunit YajC	0.34
PROKKA_04708	Esterase EstA precursor	0.34
PROKKA_03842	Outer-membrane lipoprotein LolB precursor	0.31
PROKKA_00840	Extracellular serine protease precursor	0.30
PROKKA_02401	Leukotoxin	0.30
PROKKA_03486	Aminopeptidase YwaD precursor	0.28
PROKKA_03900	Protease HtpX	0.27
PROKKA_01321	Protease PrtS precursor	0.22
PROKKA_04762	Regulator of sigma-E protease RseP	0.19
PROKKA_00839	Extracellular serine protease precursor	0.15
PROKKA_02779	Peptidase inhibitor I78 family protein	0.12
Protein synthesis		0.45
PROKKA_04929	50S ribosomal protein L21	0.37
PROKKA_05231	Bifunctional polymyxin resistance protein ArnA	0.30
PROKKA_00604	Glycine–tRNA ligase alpha subunit	0.30
Purines, pyrimidines, nucleosides, and nucleotides		
PROKKA_05372	phosphoribosylglycinamide formyltransferase	off
PROKKA_04118	allantoicase	0.20
Regulatory functions		
PROKKA_02036	Phosphoenolpyruvate synthase regulatory protein	off
PROKKA_01793	Transcriptional regulator SlyA	0.50
Signal transduction		
PROKKA_00715	Phosphate regulon sensor protein PhoR	off
PROKKA_02681	Signal transduction histidine-protein kinase BarA	off
PROKKA_03108	Methyl-accepting chemotaxis protein McpS	off
Transcription		
PROKKA_00015	DNA-directed RNA polymerase subunit beta	0.47
Transport and binding proteins		
PROKKA_00170	C4-dicarboxylate-binding periplasmic protein precursor	off
PROKKA_00278	Ferrichrome-iron receptor precursor	off
PROKKA_00710	Phosphate transport system permease protein PstA	off
PROKKA_00999	Dipeptide transport system permease protein DppC	off
PROKKA_01003	Periplasmic dipeptide transport protein precursor	off
PROKKA_01670	Ferrichrome-iron receptor precursor	off
PROKKA_02762	Ferrichrome-iron receptor precursor	off
PROKKA_02892	Arginine transport ATP-binding protein ArtM	off
PROKKA_02907	ABC transporter glutamine-binding protein GlnH precursor	off
PROKKA_03323	Biopolymer transport protein ExbB	off
PROKKA_04345	Oligopeptide-binding protein AppA precursor	off
PROKKA_04650	Hemin receptor precursor	off
PROKKA_04962	Membrane-bound lytic murein transglycosylase F precursor	off
PROKKA_05091	Aerobic C4-dicarboxylate transport protein	off
PROKKA_05128	Phosphate import ATP-binding protein PstB 3	off
PROKKA_05751	Glutathione-regulated potassium-efflux system protein KefC	off
PROKKA_01004	Periplasmic dipeptide transport protein precursor	0.49
PROKKA_00997	putative D,D-dipeptide transport ATP-binding protein DdpF	0.49
PROKKA_00544	Methionine import ATP-binding protein MetN	0.48
PROKKA_00071	putative efflux pump periplasmic linker TtgA precursor	0.48
PROKKA_01001	Periplasmic dipeptide transport protein precursor	0.48
PROKKA_03761	Hemin-binding periplasmic protein HmuT precursor	0.47
PROKKA_05370	Ferripyoverdine receptor precursor	0.42
PROKKA_01982	putative copper-importing P-type ATPase A	0.40
PROKKA_01000	Dipeptide transport system permease protein DppB	0.37
PROKKA_04423	Fe(3+) dicitrate transport protein FecA precursor	0.37
PROKKA_02687	biopolymer transport protein ExbD	0.33
PROKKA_03247	Ferric enterobactin receptor precursor	0.29
PROKKA_02904	Macrolide export protein MacA	0.28
PROKKA_00711	Phosphate import ATP-binding protein PstB	0.27
PROKKA_03129	Ferrichrome-iron receptor precursor	0.26
PROKKA_02686	Biopolymer transport protein ExbB	0.24
PROKKA_03961	Multidrug resistance protein MdtA precursor	0.23
PROKKA_00709	Phosphate transport system permease protein PstC	0.13

[a] Function predicted by Prokka annotation.
[b] "off " exclusively identified under 30 °C.

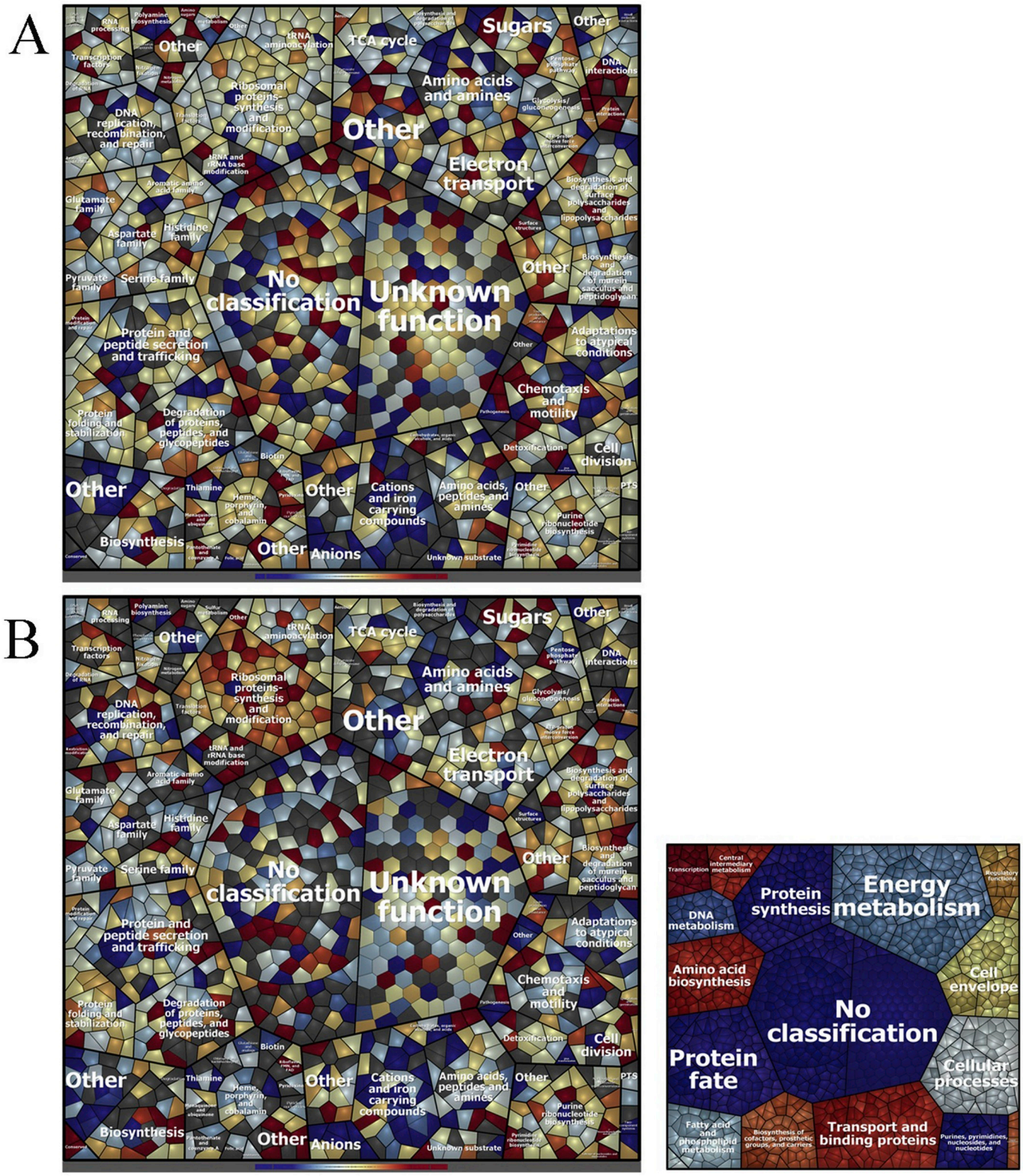

Fig. 5. Voronoi treemap visualization of *P. fluorescens* protein pattern after treatment with HLF. Proteins are depicted as single cells and grouped according to their functional classification. Classification was achieved using *Prophane 2.0* software and is based on TIGRFAMs. Large treemaps: Proteins with higher amounts in treated cells are shown in red; proteins with higher amounts in untreated cells are shown in blue. Grey cells represent proteins that were not identified in the respective condition (panel **A**: 15 °C; panel **B**: 30 °C). Small treemap represents higher level of functional classification (main role), whereas large treemaps show subrole level. (For interpretation of the references to color in this figure legend, the reader is referred to the Web version of this article.)

to the lipopolysaccharide (LPS), peptidoglycan and polyketides biosynthetic pathways (Table 1 and Supplementary Table S1). Among these we found the cellulose synthase 1 (PROKKA_04779), and Poly-beta-1,6-N-acetyl-D-glucosamine N-deacetylase precursor (PgA, PROKKA_04558) involved in biofilm formation. Conversely, filamentous hemagglutinins (PROKKA_04562; PROKKA_05581) increased

at 30 °C (Table 2).

Notably, 127 proteins with significant changes (Supplementary Table S1 and Fig. S3) does not belong to a specific functional classification or was with unknown function. At 15 °C, among unclassified proteins we found the gramicidin S synthase 2 (GbrS; PROKKA_02721) and tyrocidine synthase (TycC; PROKKA_02721), sharing 50% identity with IndC of the plant pathogen *Dickeya dadantii* 3937 (Table 1).

The list of unclassified proteins included also the hemolysin transporter protein ShlB precursor (PROKKA_04561) which increased at 30 °C (Table 2). In addition to this, other changed proteins were found involved in pathogenesis: the virulence factor Mce family protein (PROKKA_00520), leukotoxin (PROKKA_02401) and the chitinase ChiD (PROKKA_01272) differently synthesized at the two temperatures (Tables 1 and 2).

3.5. Effect of HLF-MBIC on the proteome of *P. fluorescens* ITEM 17298 planktonic cells

As depicted in Fig. 5 and Supplementary S4 significant changes were registered under HLF treatment at each temperature of incubation. Most repressed pathways included cellular processes, transport and binding, and fatty acids metabolism. Conversely, HLF treatment led to the increased amount of proteins classified in cell envelope, purines, pyrimidines, nucleosides, nucleotides and protein synthesis, and regulatory functions. A relevant percentage of varied proteins were without a functional classification or of unknown function. The deep analysis of metabolic pathways allowed to reveal main differences induced by HLF treatment.

Under treatment and regardless growth temperature no clear effect was highlighted for enzymes correlated with energy metabolism, such as Entner-Doudoroff, pentose phosphate pathways and gluconeogenesis (Tables 3 and 4, and Supplementary S2 and S3).

By contrast, the synthesis of amino acids was differently affected depending on the incubation temperature. Indeed, at 15 °C HLF-treatment favored the production of glutamate, arginine citrulline (PROKKA_03077, PROKKA_03335, PROKKA_03449, PROKKA_05608), and histidine (PROKKA_02989, PROKKA_02986, PROKKA_02987), whereas it inhibited the synthesis of aromatic amino acids from chorismate (PROKKA_00905, PROKKA_01326, PROKKA_00904, PROKKA_00895). Conversely the biosynthesis of BCAA and proline increased at 30 °C as well as those of arginine and glutamate; sulphurated amino acids and tryptophan (*via* shikimate) synthesis were repressed or completely inhibited.

Regarding the fatty acid metabolism, synthesis and catabolism were differently affected under treatment at the two temperatures of incubation (Supplementary Table S2). However, the cyclic-di-GMP-binding biofilm dispersal mediator protein, an 3-oxoacyl-[acyl-carrier-protein] reductase, catalogued in fatty acid biosynthesis was induced in treated samples under both incubation temperatures (PROKKA_02061; Table 3).

Our results suggested that under HLF treatment some modifications in the bacterial cell wall occurred; regardless of the temperature of incubation, most of ABC transporters (e.g involved in proline, histidine BCCA, phosphate and nickel uptake), TonB-dependent receptors lowered their levels or were repressed whilst, some multidrug resistance proteins were exclusively detected in treated samples (Tables 3 and 4). Interestingly, the synthesis of PROKKA_04557 and PROKKA_04558, involved respectively in the synthesis and the transport of the biofilm adhesin polysaccharide poly-beta-1,6-N-acetyl-D-glucosamine (PGA), were blocked.

Most proteins involved in regulatory functions and transcription factors underlying physiological behaviour were down regulated by the HLF-MBIC treatment. Among these, at 15 °C we found the transcriptional regulators: PROKKA_03320, the nitrogen regulator NtcA (PROKKA_01987), PROKKA_05493, PROKKA_01744, and PleD. The anti-anti-sigma factor (PROKKA_01761), PROKKA_00712,

Table 3
Proteins induced by HLF-treatment at 15 °C and 30 °C.

Identifier	Function[a]	Fold change (T/UT)[b]	
		15 °C	30 °C
Amino acid biosynthesis			
PROKKA_02989	1-(5-phosphoribosyl)-5-[(5-phosphoribosylamino) methylideneamino] imidazole-4-carboxamide isomerase	2.29	on T
PROKKA_05528	3-isopropylmalate dehydratase small subunit 1	3.79	on T
Biosynthesis of cofactors, prosthetic groups, and carriers			
PROKKA_02355	tRNA-modifying protein YgfZ	2.06	on T
PROKKA_04334	DNA nickase	2.63	on T
Cell envelope			
PROKKA_05232	Undecaprenyl-phosphate 4-deoxy-4-formamido-L-arabinose transferase	6.42	6.02
PROKKA_05226	UDP-glucose 6-dehydrogenase TuaD	on T	on T
PROKKA_02028	Outer membrane porin F precursor	3.50	2.10
PROKKA_00116	Outermembrane lipoprotein SlyB precursor	5.22	5.40
PROKKA_05229	Undecaprenyl phosphate-alpha-4-amino-4-deoxy-L-arabinose arabinosyl transferase	5.56	6.49
Cellular processes			
PROKKA_03442	UDP-4-amino-4-deoxy-L-arabinose–oxoglutarate aminotransferase	5.49	5.13
PROKKA_01782	Flagellar basal-body rod protein FlgG	on T	on T
PROKKA_00073	putative efflux pump outer membrane protein TtgC precursor	4.02	4.74
PROKKA_04999	Bacterial virulence protein (VirJ)	on T	on T
PROKKA_03935	Multidrug resistance protein MexB	3.46	3.74
Energy metabolism			
PROKKA_00423	3-mercaptopyruvate sulfurtransferase	on T	on T
PROKKA_04385	Disulfide-bond oxidoreductase YfcG	2.19	on T
PROKKA_00628	ATP synthase subunit delta	2.22	6.22
PROKKA_04874	Ferredoxin–NADP reductase	2.80	2.38
PROKKA_04485	Phosphoglycolate phosphatase	on T	on T
PROKKA_00568	5′-nucleotidase	on T	on T
Fatty acid and phospholipid metabolism			
PROKKA_02061	Cyclic-di-GMP-binding biofilm dispersal mediator protein	on T	on T
No classification			
PROKKA_00069	N-ethylmaleimide reductase	2.90	2.27
PROKKA_05230	putative 4-deoxy-4-formamido-L-arabinose phosphoundecaprenol deformylase ArnD	on T	3.13
PROKKA_05000	Phosphatidyl glycerol lysyl transferase	on T	on T
PROKKA_00573	Limonene 1,2-monooxygenase	2.98	on T
PROKKA_00705	Putative glucose-6-phosphate 1-epimerase	2.40	on T
PROKKA_05594	Polyketide cyclase/dehydrase and lipid transport	on T	on T
PROKKA_00161	MltA-interacting protein MipA	on T	on T
PROKKA_01044	Hypotheticalprotein	2.21	on T
PROKKA_01517	Hypothetical protein	4.58	on T
PROKKA_04800	Hypothetica lprotein	on T	on T
Protein fate			
PROKKA_05085	Putative signal peptide peptidase SppA	2.91	2.06
PROKKA_00645	FtsH protease regulator HflC	on T	on T
PROKKA_02543	ATP-dependent Clp protease proteolytic subunit	2.69	on T
PROKKA_04332	General stress protein 18	2.98	on T
PROKKA_01103	putative lipoprotein YiaD precursor	2.73	2.28
PROKKA_02658	Outer-membrane lipoprotein carrier protein precursor	2.35	on T
Protein synthesis			
PROKKA_03192	50S ribosomal protein L9	2.81	6.34
PROKKA_04796	tRNA threonyl carbamoyl adenosine biosynthesis protein TsaB	on T	on T
Purines, pyrimidines, nucleosides, and nucleotides			
PROKKA_05544	Formyl tetrahydrofolate deformylase	on T	on T

(*continued on next page*)

Table 3 (*continued*)

Identifier	Function[a]	Fold change (T/UT)[b]	
		15 °C	30 °C
PROKKA_01914	Phosphoribosyl formylglycin amidinecyclo-ligase	2.11	on T
Regulatory functions			
PROKKA_02350	Sigma factor AlgU negative regulatory protein	on T	on T
Transport and binding proteins			
PROKKA_03184	Iron-utilization periplasmic protein precursor	3.05	on T
PROKKA_01064	putative ABC transporter ATP-binding protein	on T	on T
PROKKA_03936	Multidrug resistance protein MexA precursor	2.35	2.99

[a] Function predicted by Prokka annotation.
[b] "on T" exclusively identified after HLF treatment.

PROKKA_01744, and PROKKA_02036 were instead negatively HLF-affected at 30 °C. The synthesis of LutR and Sigma 54 modulation protein (PROKKA_01641), Glucitol operon repressor (PROKKA_00634), and the negative regulators of alginate biosynthesis in biofilm (MucA and MucB: PROKKA_02349, PROKKA_02350) were induced at 15 °C; MucA levels increased also under higher temperature, as well as the transcriptional regulator YdfH. At 30 °C, the two-component system BarA (PROKKA_02681), involved biofilm formation via the CsrA/CsrB regulation, was repressed.

Peptidases, metalloproteases, and oxidoreductases, enzymes involved in repair processes (chaperones), degradation of misfolded proteins were found with increased levels at both temperatures in the treated samples.

HLF treatment also affected chemotaxis and flagellar assembly. In particular, at 30 °C, proteins involved in transmission of sensory signals from the chemoreceptors to the flagellar motors (PROKKA_01735, PROKKA_01742, PROKKA_05548, and PROKKA_03270) decreased their levels or they were repressed in presence of HLF. Similar response was found at 15 °C (PROKKA_05548; PROKKA_02393; PROKKA_04405, PROKKA_05339; PROKKA_01744).

Finally, a high number of uncharacterized or unclassified proteins varied under HLF treatment at each temperature (115 and 103, at 15 and 30 °C, respectively; Supplementary Table S3). Among these, proteins with lower amount after treatment included proteins involved in the synthesis of indigoidine pigment (PROKKA_02721 and PROKKA_02722).

4. Discussion

P. fluorescens exhibits a broad temperature adaptability affecting its spoilage activity mainly in cold stored foods. This behavior causes an evident competitive microbial advantage that is also favoured by biofilm formation and the ability to tackle to environmental changes. In this context, the mechanisms underlying physiological and spoilage traits of this microorganisms have been poorly studied. To this purpose, we firstly investigated strain phenotypic traits (biofilm biomass produced and formation of motility appendages) at 15 and 30 °C. These temperature values were chosen according both the optimal growth condition of this species (30 °C) and the ability of this strain to survive under cold stress, also exhibiting specific behavior, such as pigment production and biofilm formation (15 °C; Caputo et al., 2015; Chierici et al., 2016).

In this study *P. fluorescens* ITEM 17298 increased nearly twice the biofilm biomass at 15 °C, compared to that produced under higher temperature; in addition, twitching was induced in the same conditions as well as the appearance of tendrils in swimming motility. In accordance with other studies (Chierici et al., 2016; Cabrita et al., 2015), these results suggested that the low temperature favored the coordinated expression of genes and proteins involved in the lifestyle changes of this bacterium. It has been reported that flagellar motility and biofilm formation are affected by high level of c-di-GMP (Muriel et al., 2018), in turn regulated by a diguanylate cyclases with a GGDEF domain (Fazli et al., 2014). In our work, the induction of the response regulator PleD with a GGDEF domain was found at 15 °C. Thus, the role of PleD in the appearance of appendices in *P. fluorescens* swimming phenotype could not be excluded. In addition, in ITEM 17298 strain the alginate biosynthesis transcriptional regulator (AlgB) coding gene was found in the genomic locus containing PleD regulator. PleD locus also showed genetic content and organization similar to what reported for *P. aeruginosa* PAO1 and *P. fluorescens* Pf0-1 (http://www.pseudomonas.com/), thus suggesting a similar transcriptional regulation (Stover et al., 2000; Silby et al., 2009). Interestingly, at 15 °C the amount of AlgB increased by 2.8 fold compared to that found at 30 °C. The hypothesis that the low temperature promoted strain colonization was further supported by the increase of cellulose synthase 1, involved in cellulose biosynthesis.

Cellulose, alginate and poly-N-acetylglucosamine (PGA), extracellular polysaccharides of the bacterial biofilm matrix are likely synthesized and secreted by a conserved mechanism, activates by C-di-GMP levels (Morgan et al., 2014). This mechanism putatively included the carbon storage regulator (CsrA), exclusively detected in ITEM 17298 grown at 15 °C. In *E. coli* the complex protein cascade caused by CsrA culminated with the repression of the enzyme required for the synthesis of the adhesin PGA; however, in cold-adapted ITEM 17298 cells, PROKKA_04558, involved in the N-deacetylation needed for surface adhesion, was induced; thus, a complex mechanism based on the interaction among CrsA and the cold-induced RsmE, RsmD, RsmH regulators could not be excluded for this food spoiler (Kulkarni et al., 2014).

In *P. aeruginosa* CrsA also regulates the expression of LysR-type regulator (Fazli et al., 2014), required for the transcription of the *pqs*ABCDE and *phn*AB operons and the biosynthesis of signaling molecule of (PQS)-mediated *quorum sensing* (QS) (Kulkarni et al., 2014). Even though, no PQS-related genes were found in the genome of ITEM 17298, high amount of the LysR family transcriptional regulator, the unclassified PhnA (PROKKA_04927) and the enzymes linked to the QS regulation of anthranilate metabolism (PROKKA_03906, PROKKA_04397, PROKKA_03985, PROKKA_04707; PROKKA_04900) were detected at 15 °C.

Protein regulators also included the HTH-type transcriptional regulators, LutR and YdfH, belonging to the GntR family, that were exclusively detected or up-regulated at 15 °C; these proteins were previously associated to biofilm formation and antibiotic biosynthesis (İrigül-Sönmez et al., 2014). Inspection of the *P. fluorescens* LutR C-terminal domain showed a high homology with FadR-like proteins, a transcription factor that regulates the expression of genes encoding fatty acid biosynthesis; thus, LutR could be implicated in the upregulation of enzymes related to the fatty acid biosynthesis, as registered at 15 °C. The modulation of fatty acid composition is expected in order to maintain the proteins function in presence of a altered membrane fluidity under cold incubation.

In addition, in other bacteria *gntR* family transcriptional regulator was reported together with *luxR, luxI* genes as forming a QS regulated operon (Hao et al., 2010; Sakihama et al., 2012).

Likewise, genomic analysis showed genetic determinants of the QS *las, lux, rhl,* and cyclic-di-GMP systems as well as proteomic results revealed differentially expressed QS-regulated proteins (PROKKA_00428, PROKKA_04707, PROKKA_05356 at 15 °C, and PROKKA_04762, PROKKA_01619, PROKKA_00073 at 30 °C). This cell-to cell communication could be at the basis of the bacterial spoilage (proteolysis, lipolysis) of some food products (Bai and Rai, 2011); thus, understanding bacterial QS or the regulated phenotypic traits (biofilm)

Table 4
Proteins repressed by HLF-treatment at 15 °C and 30 °C.

Identifier	Function[a]	Fold change (T/UT)[b]	
		15 °C	30 °C
Amino acid biosynthesis			
PROKKA_00203	Cystathionine beta-lyase	0.23	off T
PROKKA_01787	Aspartate aminotransferase	0.45	0.48
Biosynthesis of cofactors, prosthetic groups, and carriers			
PROKKA_03463	Omega-amino acid–pyruvate aminotransferase	0.28	0.18
PROKKA_03147	Phosphomethylpyrimidine synthase	off T	off T
PROKKA_02039	putative adenylyltransferase/ sulfurtransferase MoeZ	off T	off T
Cell envelope			
PROKKA_04557	Poly-beta-1,6-N-acetyl-D-glucosamine export protein precursor	off T	off T
Cellular processes			
PROKKA_00897	UDP-2-acetamido-2-deoxy-3-oxo-D-glucuronate aminotransferase	off T	off T
PROKKA_00898	UDP-2-acetamido-2-deoxy-3-oxo-D-glucuronate aminotransferase	off T	off T
PROKKA_05548	Methyl-accepting chemotaxis protein PctA	off T	0.34
PROKKA_04511	ComE operon protein 1	off T	off T
PROKKA_00251	Acyl-homoserine lactone acylasePvdQ precursor	off T	off T
PROKKA_01272	Chitinase D precursor	off T	off T
Central intermediary metabolism			
PROKKA_02553	Carbon-nitrogen hydrolase	off T	off T
DNA metabolism			
PROKKA_04783	Major cold shock protein CspA	off T	off T
Energy metabolism			
PROKKA_03027	Imidazolone propionase	off T	off T
PROKKA_01666	Ureidoglycolate lyase	off T	off T
PROKKA_03025	Histidine ammonia-lyase	0.23	0.31
PROKKA_00268	Glutathione S-transferase GstB	0.46	0.44
PROKKA_05600	Aminomethyl transferase	0.19	0.47
PROKKA_00695	Aspartateammonia-lyase	0.35	0.50
PROKKA_04586	Cytochrome c	off T	0.10
PROKKA_05220	putative enoyl-CoA hydratase echA8	0.29	0.10
PROKKA_03584	putative enoyl-CoA hydratase 1	0.09	0.18
PROKKA_02048	Methylisocitrate lyase	0.14	0.19
PROKKA_02580	Hydroxycinnamoyl-CoAhydratase-lyase	off T	0.21
PROKKA_00641	Phospholipase YtpA	off T	0.23
PROKKA_05262	Methionyl-tRNA formyltransferase	0.21	0.32
PROKKA_02508	Lipoamide acyltransferase component of branched-chain alpha-keto acid dehydrogenase complex	off T	0.12
PROKKA_02639	Isocitrate lyase	0.25	0.30
PROKKA_01237	Fumarate hydratase class II	0.43	0.42
Fatty acid and phospholipid metabolism			
PROKKA_05217	3-oxoacyl-[acyl-carrier-protein] reductase FabG	0.13	0.17
PROKKA_05216	Acetyl-coenzyme A synthetase	off T	off T
PROKKA_00502	Acyl-CoA dehydrogenase	off T	off T
PROKKA_02582	Acyl-CoA dehydrogenase	off T	0.17
PROKKA_01442	putative succinyl-CoA:3-ketoacid coenzyme A transferase subunit A	off T	0.32
PROKKA_01803	Putative outer membrane protein precursor	0.48	0.41
PROKKA_05661	Long-chain-fatty-acid–CoA ligase	0.13	0.43
No classification			
PROKKA_05738	Nucleoside-specific channel-forming protein tsx precursor	off T	off T
PROKKA_00717	Secreted repeat of unknown function	off T	off T
PROKKA_03447	CYTH domain protein	off T	off T
PROKKA_00834	Serralysin precursor	off T	off T
PROKKA_04692	PrkA AAA domain protein	0.48	0.19
PROKKA_00895	Indole-3-glycerol phosphate synthase	off T	0.21
PROKKA_04821	Inner membrane protein YebE	0.46	0.41
PROKKA_05559	Porin D precursor	0.30	0.45
PROKKA_01146	Serine 3-dehydrogenase	off T	0.48
PROKKA_05645	putative sugar-binding periplasmic protein precursor	0.32	0.48
PROKKA_03131	Decarbamoyl novobiocin carbamoyltransferase	0.37	0.49
PROKKA_02387	Hypothetical protein	off T	off T
PROKKA_04269	Hypotheticalprotein	off T	off T
PROKKA_05138	Hypothetical protein	off T	off T
PROKKA_05429	Hypothetical protein	off T	off T
PROKKA_01958	Hypothetical protein	off T	0.06
PROKKA_01096	Hypothetical protein	0.04	0.17
PROKKA_04669	Hypothetical protein	off T	0.23
PROKKA_01095	Hypothetical protein	off T	0.24
PROKKA_04341	Hypothetical protein	0.35	0.30
PROKKA_04546	Hypothetical protein	0.14	0.39
PROKKA_04556	Hypothetical protein	0.47	0.44
Protein fate			
PROKKA_01321	Protease PrtS precursor	off T	off T
PROKKA_00900	putative succinyl-diaminopimelate desuccinylase	off T	off T
PROKKA_05384	Carboxypeptidase G2 precursor	off T	0.46
PROKKA_01697	Extracellular serine protease precursor	off T	off T
PROKKA_00839	Extracellular serine protease precursor	off T	off T
PROKKA_00840	Extracellular serine protease precursor	off T	0.09
PROKKA_03486	Aminopeptidase YwaD precursor	off T	0.11
PROKKA_04761	Outer membrane protein assembly factor BamA precursor	0.40	0.23
PROKKA_04708	Esterase EstA precursor	off T	0.24
Protein synthesis			
PROKKA_00026	30S ribosomal protein S19	off T	off T
Purines, pyrimidines, nucleosides, and nucleotides			
PROKKA_04118	allantoicase	0.42	0.06
PROKKA_03623	AMP nucleosidase	0.48	0.34
Regulatory functions			
PROKKA_00716	Phosphate regulon transcriptional regulatory protein PhoB	off T	off T
Transport and binding proteins			
PROKKA_00340	Glycine betaine-binding protein OpuAC precursor	off T	off T
PROKKA_02443	Glycine betaine-binding protein OpuAC precursor	0.48	off T
PROKKA_00101	Leucine-, isoleucine-, valine-, threonine-, and alanine-binding protein precursor	0.19	0.25
PROKKA_00709	Phosphate transport system permease protein PstC	off T	off T
PROKKA_05125	Phosphate-binding protein PstS precursor	0.21	0.10
PROKKA_00708	Phosphate-binding protein PstS precursor	0.08	0.12
PROKKA_00711	Phosphate import ATP-binding protein PstB	off T	0.12
PROKKA_05370	Ferripyoverdine receptor precursor	off T	off T
PROKKA_04201	Oligopeptide-binding protein AppA precursor	off T	off T
PROKKA_04286	putative TonB-dependent receptor BfrD precursor	off T	off T
PROKKA_05140	Magnesium-transporting ATPase, P-type 1	0.07	0.10
PROKKA_04423	Fe(3+) dicitrate transport protein FecA precursor	off T	0.16
PROKKA_01001	Periplasmic dipeptide transport protein precursor	0.10	0.22
PROKKA_00997	putative D,D-dipeptide transport ATP-binding protein DdpF	off T	0.46
PROKKA_04604	putative periplasmic iron-binding protein precursor	off T	off T

[a] Function predicted by Prokka annotation.
[b] "off T" exclusively identified under control condition.

can help in deciphering population dynamics in cold stored foods and in controlling the growth of undesirable food-related bacteria.

During food storage, spoilage bacteria can release polyamines, considered markers of spoilage degree, and harmful to human health at high concentrations (Shalaby, 1996). In bacterial cells polyamines are organic polycationic molecules playing a crucial role both in modulate biofilm formation (Karatan and Watnick, 2009) and in DNA metabolism (Venancio-Marques et al., 2014). Interestingly, in ITEM 17298 under low temperature, the arginine metabolism was favored to produce polyamines and glutamate; the high amount of enzymes involved in polyamine synthesis could be correlated with the induced proteins involved in DNA replication, transcription and translation, and protein synthesis; these latter pathways probably sustained the cold adaptive bacterial response, as previously reported (Iost et al., 2013).

Mechanisms of adaptation to low temperature also involved the iron uptake; indeed, in ITEM 17298 at 15 °C proteins responsible for iron recovery and storage were exclusively detected up-regulated; these data suggested that the storing of this nutrient occurred in response to a higher demand for metabolic energy (Dhungana et al., 2003) or to counteract oxidative damage (Ma et al., 1999); this latter condition was sustained by the increase in the levels of proteins responsible for repair and defense mechanisms (PROKKA_03320, PROKKA_03674, PROKKA_05169, PROKKA_03672, PROKKA_04041, PROKKA_03426).

In light of these results, it can be suposed that cellular mechanisms, here for the first time investigated, could be responsible for strain adaptation and persistence under the low temperature, also making it difficult to control their spread in the food chain.

Recently, antimicrobial peptides (AMPs) have shown good anti-biofilm activity at the point of being considered as promising therapeutic agents in human infection (Batoni et al., 2016). In this study, the sub-lethal concentration of pepsin digested bovine lactoferrin (HLF; *ca.* 17-fold lower than that used for its antimicrobial activity in cold-stored cheese; Caputo et al., 2015), significantly reduced biofilm formation at the assayed temperatures; swimming and twitching motility were mostly affected at 15 °C and tendrils were inhibited in a dose-dependent manner. Thus, in accordance with other studies (Ho et al., 2012), these results sustained the hypothesis that BLF-derived peptides penetrated the cell membrane and affected intracellular targets.

Indeed, proteomic analysis revealed that the PleD regulator was absent under HLF treatment at 15 °C, whilst the negative AlgB regulators (MucA and MucB) were induced in the treated samples at both temperatures; the synthesis of these transcriptional factors inhibited the conversion from a non-mucoid to a mucoid phenotype of *P. fluorescens* and *P. aeruginosa* (Ahmed, 2007). Likewise, HLF treatment inhibited the 30°C-induced adhesion factor filamentous hemagglutinin in accordance with previous results (Di Biase et al., 2004). The cyclic-di-GMP-binding biofilm dispersal mediator protein (PROKKA_02061) was also detected in all treated samples; as reported for other species, this protein reduced c-di-GMP causing biofilm dispersal (Ma et al., 2011).

The low temperature favored the synthesis of proteins involved in the response to oxidative stress in the untreated samples. Interestingly, these protein (PROKKA_03320, PROKKA_03674, PROKKA_04041) were repressed in all treated-HLF samples. Similar effects were registered for the TonB-dependent receptors and PvdQ, involved in the synthesis of the siderophore pyoverdine and degradation of QS molecules (3-oxo-C_{12}-homoserine lactone); by contrast, proteins responsible for iron storage were up-regulated. Recently, modulators of oxidative stress response and iron acquisition have been proposed as a suitable strategy to reduce *P. aeruginosa* virulence and persistence (Sethupathy et al., 2016; Wurst et al., 2014) and therefore could be also exploited to counteract *P. fluorescens* spread in the refrigerated food and environments.

In our previous study, we reported the finding of the pigment leuco-indigoidine in cold-stored mozzarella cheese inoculated with ITEM 17298; this compound is the reduced form of the reactive blue pigment indigoidine (Caputo et al., 2015). Our research demonstrated that the treatment with HLF inhibited pigment release throughout the entire refrigerated period. Although Andreani et al. (2015) suggested that the blue pigment was not indigoidine, in this study PROKKA_02721 and PROKKA_02722 proteins correlated with the synthesis of this pigment were found at 15 °C. These proteins are non-ribosomal peptide synthetases subdivided into domains responsible for substrate adenylation, thiolation and condensation that culminated in pigment biosynthesis. A conserved core motif (DNFFELGGHSL) similar to that found in the thiolation (T) domain of *S. chromofuscus* (DDFFELGGNSL; Yu et al., 2013) was also shown. In this last species the stability of the modular indigoidine synthase Sc-IndC and the product indigoidine was attributed to the optimal temperature of 18 °C. In addition, in *D. dadantii* 3937, IndC synthesizes the blue pigment indigoidine together with the pantetheine-phosphate adenylyltransferase (CoaD; Reverchon et al., 2002), also cold-induced in our target strain (PROKKA_00418). Even though the biosynthetic pathway of indigoidine has been proposed for other microorganisms, the specific role of this pigment and its regulation, including *luxRI* quorum sensing regulators, have been only touched (Yu et al., 2013; Cude et al., 2015).

5. Conclusion

For the first time the proteome profile of a blue pigmenting and biofilm forming *P. fluorescens* was presented in this work. Proteomic results were consistent with microbiological ones favoring at the low temperature both the highest biofilm biomass and an increase of different protein determinants related with biofilm formation, cell motility, and adhesion. Conversely, at 30 °C some virulence factors such as leukotoxin were detected, highlighting the need to further investigate this strain.

Notably, a high percentage of proteins with relevant changes in amount was without a specific functional classification or of unknown function; among these latter, for the first time, we identified enzymes related to the blue pigment indigoidine that was produced at low temperature.

This work also proposes a strategy based on the application of milk protein-derived peptides to hamper biofilm formation by this food spoiler. Indeed, by using a sublethal HLF concentration, proteins involved in biofilm regulation and exopolysaccharide synthesis were repressed at 15 °C, whilst the cyclic-di-GMP-binding biofilm dispersal mediator was instead detected at both temperatures. In addition, HLF treatment inhibited indigoidine synthesis related enzymes involved in blue cheese discoloration and reduction of shelf life of cold stored cheeses.

Author contributions

LQ, KR designed research; FF, VCL performed genomic analysis; LQ, DZ performed proteomic analysis; DB and CH performed mass spectrometry analyses; LQ and LC performed and analyzed microbiological data; LQ and DZ analyzed proteomic data; LQ and DZ wrote the paper; LQ, DZ, AFL, LC, FF and KR revised the manuscript.

The authors are thankful to Dr Lucia Decastelli (Istituto Zooprofilattico Sperimentale del Piemonte, Liguria 62 e Valle d'Aosta, Turin, Italy) for having supplied the strain used in this study.

Appendix A. Supplementary data

Supplementary data to this article can be found online at https://doi.org/10.1016/j.fm.2019.02.003.

Funding

The research was funded by National Research Council (CNR), Italy through the Short-Term Mobility programme for the year 2016.

References

Ahmed, N., 2007. Genetics of bacterial alginate: alginate genes distribution, organization and biosynthesis in bacteria. Curr. Genom. 8 (3), 191–202.

Andreani, N.A., Carraro, L., Martino, M.E., Fondi, M., Fasolato, L., Miotto, G., Magro, M., Vianello, F., Cardazzo, B., 2015. A genomic and transcriptomic approach to investigate the blue pigment phenotype in *Pseudomonas fluorescens*. Int. J. Food Microbiol. 213, 88–98.

Bai, A.J., Rai, V.R., 2011. Bacterial quorum sensing and food industry. Compr. Rev. Food Sci. Food Saf. 10 (3), 183–193.

Baruzzi, F., Lagonigro, R., Quintieri, L., Morea, M., Caputo, L., 2012. Occurrence of non-lactic acid bacteria populations involved in protein hydrolysis of cold-stored high moisture Mozzarella cheese. Food Microbiol. 30 (1), 37–44.

Baruzzi, F., Pinto, L., Quintieri, L., Carito, A., Calabrese, N., Caputo, L., 2015. Efficacy of lactoferricin B in controlling ready-to-eat vegetable spoilage caused by *Pseudomonas* spp. Int. J. Food Microbiol. 215, 179–186.

Batoni, G., Maisetta, G., Esin, S., 2016. Antimicrobial peptides and their interaction with biofilms of medically relevant bacteria. Biochim. Biophys. Acta Biomembr. 1858 (5), 1044–1060.

Cabrita, P., Trigo, M.J., Ferreira, R.B., Brito, L., 2015. Differences in the expression of cold stress–related genes and in the swarming motility among persistent and sporadic strains of *Listeria monocytogenes*. Foodb. Pathog. Dis. 12 (7), 576–584.

Caldera, L., Franzetti, L., Van Coillie, E., De Vos, P., Stragier, P., De Block, J., Heyndrickx, M., 2016. Identification, enzymatic spoilage characterization and proteolytic activity quantification of *Pseudomonas* spp. isolated from different foods. Food Microbiol. 54, 142–153.

Caputo, L., Quintieri, L., Bianchi, D.M., Decastelli, L., Monaci, L., Visconti, A., Baruzzi, F., 2015. Pepsin-digested bovine lactoferrin prevents Mozzarella cheese blue discoloration caused by *Pseudomonas fluorescens*. Food Microbiol. 46, 15–24.

Caputo, L., Quintieri, L., Cavalluzzi, M.M., Lentini, G., Habtemariam, S., 2018. Antimicrobial and antibiofilm activities of citrus water-extracts obtained by microwave-assisted and conventional methods. Biomedicines 6 (2).

Chierici, M., Picozzi, C., La Spina, M.G., Orsi, C., Vigentini, I., Zambrini, V., Foschino, R., 2016. Strain Diversity of *Pseudomonas fluorescens* group with potential blue pigment phenotype isolated from dairy products. J. Food Protect. 79 (8), 1430–1435.

Cude, W.N., Prevatte, C.W., Hadden, M.K., May, A.L., Smith, R.T., Swain, C.L., Campagna, S.R., Buchan, A., 2015. *Phaeobacter* sp. strain Y4I utilizes two separate cell-to-cell communication systems to regulate production of the antimicrobial indigoidine. Appl. Environ. Microbiol. 81 (4), 1417–1425.

Deziel, E., Comeau, Y., Villemur, R., 2001. Initiation of biofilm formation by *Pseudomonas aeruginosa* 57RP correlates with emergence of hyperpiliated and highly adherent phenotypic variants deficient in swimming, swarming, and twitching motilities. J. Bacteriol. 183 (4), 1195–1204.

Dhungana, S., Taboy, C.H., Anderson, D.S., Vaughan, K.G., Aisen, P., Mietzner, T.A., Crumbliss, A.L., 2003. The influence of the synergistic anion on iron chelation by ferric binding protein, a bacterial transferring. Proc. Natl. Acad. Sci. U.S.A. 100 (7), 3659–3664.

Di Biase, A.M., Tinari, A., Pietrantoni, A., Antonini, G., Valenti, P., Conte, M.P., Superti, F., 2004. Effect of bovine lactoferricin on enteropathogenic *Yersinia* adhesion and invasion in HEp-2 cells. J. Medical Microbiol 53 (5), 407–412.

Dickson, R.P., Erb-Downward, J.R., Freeman, C.M., Walker, N., Scales, B.S., Beck, J.M., Martinez, F.J., Curtis, V.N., Lama, V.N., Huffnagle, G.B., 2014. Changes in the lung microbiome following lung transplantation include the emergence of two distinct *Pseudomonas* species with distinct clinical associations. PLoS One 9 (5), e97214.

Donnarumma, G., Buommino, E., Fusco, A., Paoletti, I., Auricchio, L., Tufano, M.A., 2010. Effect of temperature on the shift of *Pseudomonas fluorescens* from an environmental microorganism to a potential human pathogen. Int. J. Immunopathol. Pharmacol. 23 (1), 227–234.

Fanelli, F., Liuzzi, V.C., Quintieri, L., Mulè, G., Baruzzi, F., Logrieco, A.F., Caputo, L., 2017. Draft genome sequence of the cheese spoilage *Pseudomonas fluorescens* ITEM 17298. Genome Announc. 5 e01141-17.

Fazli, M., Almblad, H., Rybtke, M.L., Givskov, M., Eberl, L., Tolker-Nielsen, T., 2014. Regulation of biofilm formation in *Pseudomonas* and *Burkholderia* species. Environ. Microbiol. 16 (7), 1961–1981.

Grube, M., Cernava, T., Soh, J., Fuchs, S., Aschenbrenner, I., Lassek, C., Wegner, U., Becher, D., Riedel, K., Sensen, C.W., Berg, G., 2015. Exploring functional contexts of symbiotic sustain within lichen-associated bacteria by comparative omics. ISME J. 9 (2), 412–424.

Hao, Y., Winans, S.C., Glick, B.R., Charles, T.C., 2010. Identification and characterization of new LuxR/LuxI-type *quorum sensing* systems from metagenomic libraries. Environ. Microbiol. 12 (1), 105–117.

Hentzer, M., Wu, H., Andersen, J.B., Givskov, M., 2003. Attenuation of *Pseudomonas aeruginosa* virulence by *quorum sensing* inhibitors. EMBO J. 22 (15), 3803–3815.

Ho, Y.H., Sung, T.C., Chen, C.S., 2012. Lactoferricin B inhibits the phosphorylation of the two-component system response regulators BasR and CreB. Mol. Cell. Proteomics 11 (4) M111-014720.

Iost, I., Bizebard, T., Dreyfus, M., 2013. Functions of DEAD-box proteins in bacteria: current knowledge and pending questions. Biochim. Biophys. Acta 1829 (8), 866–877.

İrigül-Sönmez, Ö., Köroğlu, T.E., Öztürk, B., Kovács, Á.T., Kuipers, O.P., Yazgan-Karataş, A., 2014. In *Bacillus subtilis* LutR is part of the global complex regulatory network governing the adaptation to the transition from exponential growth to stationary phase. Microbiol. 160 (2), 243–260.

Karatan, E., Watnick, P., 2009. Signals, regulatory networks, and materials that build and break bacterial biofilms. Microbiol. Mol. Biol. Rev. 73 (2), 310–347.

Khan, M.S.A., Zahin, M., Hasan, S., Husain, F.M., Ahmad, I., 2009. Inhibition of quorum sensing regulated bacterial functions by plant essential oils with special reference to clove oil. Lett. Appl. Microbiol. 49 (3), 354–360.

Kulkarni, P.R., Jia, T., Kuehne, S.A., Kerkering, T.M., Morris, E.R., Searle, M.S., Heeb, S., Rao, J., Kulkarni, R.V., 2014. A sequence-based approach for prediction of CsrA/RsmA targets in bacteria with experimental validation in *Pseudomonas aeruginosa*. Nucleic Acids Res. 42 (11), 6811–6825.

López-Mondéjar, R., Zühlke, D., Becher, D., Riedel, K., Baldrian, P., 2016. Cellulose and hemicellulose decomposition by forest soil bacteria proceeds by the action of structurally variable enzymatic systems. Sci. Rep. 6, 25279.

Lundgren, D.H., Martinez, H., Wright, M.E., Han, D.K., 2009. Protein identification using Sorcerer 2 and SEQUEST. Curr. Protoc. Bioinformatics. 13, 3.

Ma, J.F., Ochsner, U.A., Klotz, M.G., Nanayakkara, V.K., Howell, M.L., Johnson, Z., Posey, J.E., Vasil, M.L., Monaco, J.J., Hassett, D.J., 1999. Bacterioferritin A modulates catalase A (KatA) activity and resistance to hydrogen peroxide in *Pseudomonas aeruginosa*. J. Bacteriol. 181 (12), 3730–3742.

Ma, Q., Yang, Z., Pu, M., Peti, W., Wood, T.K., 2011. Engineering a novel c-di-GMP-binding protein for biofilm dispersal. Environ. Microbiol. 13 (3), 631–642.

Madi, A., Lakhdari, O., Blottière, H.M., Guyard-Nicodeme, M., Le Roux, K., Groboillot, A., Svinareff, P., Doré, J., Orange, N., Feuilloley, M.G., Connil, N., 2010. The clinical *Pseudomonas fluorescens* MFN1032 strain exerts a cytotoxic effect on epithelial intestinal cells and induces Interleukin-8 via the AP-1 signaling pathway. BMC Microbiol. 10, 215.

Mavrodi, D.V., Parejko, J.A., Mavrodi, O.V., Kwak, Y.S., Weller, D.M., Blankenfeldt, W., Thomashow, L.S., 2013. Recent insights into the diversity, frequency and ecological roles of phenazines in fluorescent *Pseudomonas* spp. Environ. Microbiol. 15 (3), 675–686.

Monds, R.D., O'Toole, G.A., 2009. The developmental model of microbial biofilms: ten years of a paradigm up for review. Trends Microbiol. 17 (2), 73–87.

Morgan, J.L., McNamara, J.T., Zimmer, J., 2014. Mechanism of activation of bacterial cellulose synthase by cyclic di-GMP. Nat. Struct. Mol. Biol. 21 (5), 489.

Morici, P., Fais, R., Rizzato, C., Tavanti, A., Lupetti, A., 2016. Inhibition of *Candida albicans* biofilm formation by the synthetic lactoferricin derived peptide hlf1-11. PLoS One 11 (11), e0167470.

Muriel, C., Arrebola, E., Redondo-Nieto, M., Martínez-Granero, F., Jalvo, B., Pfeilmeier, S., Blanco-Romero, E., Baena, I., Malone, J.G., Rivilla, R., Martín, M., 2018. AmrZ is a major determinant of c-di-GMP levels in *Pseudomonas fluorescens* F113. Sci. Rep. 8 (1), 1979.

Naghmouchi, K., Le Lay, C., Baah, J., Drider, D., 2012. Antibiotic and antimicrobial peptide combinations: synergistic inhibition of *Pseudomonas fluorescens* and antibiotic-resistant variants. Res. Microbiol. 163 (2), 101–108.

Nishimura, T., Hattori, K., Inoue, A., Ishii, T., Yumoto, T., Tsukahara, K., Nakao, A., Ishihara, S., Nakayama, S., 2017. Bacteremia or pseudobacteremia? Review of pseudomonas fluorescens infections. West. J. Emerg. Med. 8 (2), 151–154.

O'Toole, G.A., 2011. Microtiter dish biofilm formation assay. JoVE(47) e2437-e2437.

Oliveira, N.M., Martinez-Garcia, E., Xavier, J., Durham, W.M., Kolter, R., Kim, W., Foster, K.R., 2015. Biofilm formation as a response to ecological competition. PLoS Biol. 13 (7), e1002191.

Park, A.J., Murphy, K., Krieger, J.R., Brewer, D., Taylor, P., Habash, M., Khursigara, C.M., 2014. A temporal examination of the planktonic and biofilm proteome of whole cell *Pseudomonas aeruginosa* PAO1 using quantitative mass spectrometry. Mol. Cell. Proteomics 13 (4), 1095–1105.

Quintieri, L., Caputo, L., Monaci, L., Deserio, D., Morea, M., Baruzzi, F., 2012. Antimicrobial efficacy of pepsin-digested bovine lactoferrin on spoilage bacteria contaminating traditional mozzarella cheese. Food Microbiol. 31, 64–71.

Quintieri, L., Caputo, L., Morea, M., Baruzzi, F., 2013a. Control of Mozzarella spoilage bacteria by using bovine lactoferrin pepsin-digested hydrolysate. In: Mendèz-Vilas, A. (Ed.), Worldwide Research Efforts in the Fighting against Microbial Pathogens: from Basic Research to Technological Developments. BrownWalker Press, Boca Raton, FL, USA, pp. 118–122.

Quintieri, L., Pistillo, B.R., Caputo, L., Favia, P., Baruzzi, F., 2013b. Bovine lactoferrin and lactoferricin on plasma-deposited coating against spoilage *Pseudomonas* spp. Innov. Food Sci. Emerg. Technol. 20, 215–222.

Quintieri, L., Carito, A., Pinto, L., Calabrese, N., Baruzzi, F., Caputo, L., 2015. Application of lactoferricin B to control microbial spoilage in cold stored fresh foods. In: Mendèz-Vilas, A. (Ed.), "Multidisciplinary Approach for Studying and Combating Microbial Pathogens", Microbiology Series Volume 3. BrownWalker Press, pp. 58–62.

Rajput, A., Kumar, M., 2018. Anti-biofilm peptides: a new class of quorum quenchers and their prospective therapeutic applications. In: Biotechnological Applications of Quorum Sensing Inhibitors. Springer, Singapore, pp. 87–110.

Reverchon, S., Rouanet, C., Expert, D., Nasser, W., 2002. Characterization of indigoidine biosynthetic genes in *Erwinia chrysanthemi* and role of this blue pigment in pathogenicity. J. Bacteriol. 184 (3), 654–665.

Rossi, C., Serio, A., Chaves-López, C., Anniballi, F., Auricchio, B., Goffredo, E., Cenci-Goga, B.T., Lista, F., Fillo, S., Paparella, A., 2018. Biofilm formation, pigment production and motility in *Pseudomonas* spp. isolated from the dairy industry. Food Control 86, 241–248.

Saeed, A.I., Sharov, V., White, J., White, J., Li, J., Liang, W., Bhagabati, N., Braisted, J., Klapa, M., Currier, T., Thiagarajan, M., Sturn, A., Snuffin, M., Rezantsev, A., Popov, D., Ryltsov, A., Kostukovich, E., Borisovsky, I., Liu, Z., Vinsavich, A., Trush, V., Quackenbush, J., 2003. TM4: a free, open-source system for microarray data management and analysis. Biotechnologia 34, 374–378.

Sakihama, Y., Mizoguchi, H., Oshima, T., Ogasawara, N., 2012. YdfH identified as a repressor of rspA by the use of reduced genome *Escherichia coli* MGF-01. Biosci. Biotechnol. Biochem. 76 (9), 1688–1693.

Sánchez-Gómez, S., Ferrer-Espada, R., Stewart, P.S., Pitts, B., Lohner, K., Martínez de

Tejada, G., 2015. Antimicrobial activity of synthetic cationic peptides and lipopeptides derived from human lactoferricin against *Pseudomonas aeruginosa* planktonic cultures and biofilms. BMC Microbiol. 15 (1), 137.
Seemann, T., 2014. Prokka: rapid prokaryotic genome annotation. Bioinformation 30 (14), 2068–2069.
Sethupathy, S., Prasath, K.G., Ananthi, S., Mahalingam, S., Balan, S.Y., Pandian, S.K., 2016. Proteomic analysis reveals modulation of iron homeostasis and oxidative stress response in *Pseudomonas aeruginosa* PAO1 by curcumin inhibiting quorum sensing regulated virulence factors and biofilm production. J. Proteomics 145, 112–126.
Shalaby, A.R., 1996. Significance of biogenic amines to food safety and human health. Food Res. Int. 29 (7), 675–690.
Silby, M.W., Cerdeño-Tárraga, A.M., Vernikos, G.S., Giddens, S.R., Jackson, R.W., Preston, G.M., Zhang, X.X., Moon, C.D., Gehrig, S.M., Godfrey, S.A., Knight, C.G., Malone, J.G., Robinson, Z., Spiers, A.J., Harris, S., Challis, G.L., Yaxley, A.M., Harris, D., Seeger, K., Murphy, L., Rutter, S., Squares, R., Quail, M.A., Saunders, E., Mavromatis, K., Brettin, T.S., Bentley, S.D., Hothersall, J., Stephens, E., Thomas, C.M., Parkhill, J., Levy, S.B., Rainey, P.B., Thomson, N.R., 2009. Genomic and genetic analyses of diversity and plant interactions of *Pseudomonas fluorescens*. Genome Biol. 10 (5) R51.
Srey, S., Jahid, I.K., Ha, S.D., 2013. Biofilm formation in food industries: a food safety concern. Food Control 31 (2), 572–585.
Stover, C.K., Pham, X.Q., Erwin, A.L., Mizoguchi, S.D., Warrener, P., Hickey, M.J., Brinkman, F.S., Hufnagle, W.O., Kowalik, D.J., Lagrou, M., Garber, R.L., Goltry, L., Tolentino, E., Westbrock-Wadman, S., Yuan, Y., Brody, L.L., Coulter, S.N., Folger, K.R., Kas, A., Larbig, K., Lim, R., Smith, K., Spencer, D., Wong, G.K., Wu, Z., Paulsen, I.T., Reizer, J., Saier, M.H., Hancock, R.E., Lory, S., Olson, M.V., 2000. Complete genome sequence of *Pseudomonas aeruginosa* PAO1: an opportunistic pathogen. Nature 406, 959–964.
Venancio-Marques, A., Bergen, A., Rossi-Gendron, C., Rudiuk, S., Baigl, D., 2014. Photosensitive polyamines for high-performance photocontrol of DNA higher-order structure. ACS Nano 8 (4), 3654–3663.
Vizcaíno, J.A., Csordas, A., del-Toro, N., Dianes, J.A., Griss, J., Lavidas, I., Hermjakob, H., 2016. 2016 update of the PRIDE database and its related tools. Nucleic Acids Res. 44 (22), 11033.
Waite, R.D., Papakonstantinopoulou, A., Littler, E., Curtis, M.A., 2005. Transcriptome analysis of *Pseudomonas aeruginosa* growth: comparison of gene expression in planktonic cultures and developing and mature biofilms. J. Bacteriol. 187 (18), 6571–6576.
Winsor, G.L., Lam, D.K., Fleming, L., Lo, R., Whiteside, M.D., Yu, N.Y., Hancock, R.E., Brinkman, F.S., 2010. *Pseudomonas* genome database: improved comparative analysis and population genomics capability for *Pseudomonas* genomes. Nucleic Acids Res. 39, D596–D600.
Wurst, J.M., Drake, E.J., Theriault, J.R., Jewett, I.T., VerPlank, L., Perez, J.R., Munoz, B., 2014. Identification of inhibitors of PvdQ, an enzyme involved in the synthesis of the siderophore pyoverdine. ACS Chem. Biol. 9 (7), 1536–1544.
Xu, G., Xiong, W., Hu, Q., Zuo, P., Shao, B., Lan, F., Lu, X., Xu, Y., Xiong, S., 2010. Lactoferrin-derived peptides and Lactoferricin chimera inhibit virulence factor production and biofilm formation in *Pseudomonas aeruginosa*. J. Appl. Microbiol. 109 (4), 1311–1318.
Yu, D., Xu, F., Valiente, J., Wang, S., Zhan, J., 2013. An indigoidine biosynthetic gene cluster from *Streptomyces chromofuscus* ATCC 49982 contains an unusual IndB homologue. J. Ind. Microbiol. Biotechnol. 40 (1), 159–168.
Zybailov, B., Mosley, A.L., Sardiu, M.E., Coleman, M.K., Florens, L., Washburn, M.P., 2006. Statistical analysis of membrane proteome expression changes in *Saccharomyces cerevisiae*. J. Proteome Res. 5 (9), 2339–2347.